Ether Oxides: A New Class of Stable Ylides? A Theoretical Study of Methanol Oxide and Dimethyl Ether Oxide

Christoph A. Schalley, Jeremy N. Harvey, Detlef Schröder, and Helmut Schwarz*

Institut für Organische Chemie der Technischen Universität, Strasse des 17. Juni 135, D-10623 Berlin, Germany

Received: September 12, 1997; In Final Form: November 19, 1997

The potential energy surfaces of neutral methanol oxide and dimethyl ether oxide and their anion and cation radicals have been calculated at the BECKE3LYP/6-311++G(d,p) level of theory. Both neutral singlet methanol and dimethyl ether oxides are predicted to correspond to local minima on their potential energy surfaces. Natural bonding orbital (NBO) population analysis reveals a distinct ylidic character for these species. Upon increasing methyl substitution, the R_2O^+—O^- ylide structure is stabilized energetically because of the better charge distribution of the formally positive central oxygen atom; thus, the energy differences relative to the $R_2O + {}^3O$ exit channel decrease significantly. The barrier for the 1,2-hydrogen migration in methanol oxide to yield methyl hydroperoxide amounts to only 5 kcal/mol, whereas the methyl shift in dimethyl ether oxide to afford dimethyl peroxide demands >40 kcal/mol and can proceed by retention or inversion of the configuration at the migrating carbon. The kinetic stabilization of the latter is instead determined either by the loss of a methyl radical or by spin crossing to the triplet surface followed by O atom loss. For this process, the minimal-energy crossing point of the two neutral surfaces was located. The corresponding cation radicals of methanol and dimethyl ether oxide rest in rather deep wells, and their geometries are not too different from those of the neutrals. Therefore, neutralization-reionization mass spectrometry may allow generation and identification of the neutral species, provided that the cation-radical precursors can be made. Furthermore, the kinetic stability of neutral dimethyl ether oxide may be sufficient for its detection in matrix isolation experiments.

Introduction

Neutral singlet water oxide has attracted much attention during the last three decades. This elusive molecule is not only of academic interest because of its hypervalent,[1] ylidic H_2O^+—O^- structure, but has also been postulated as a possible intermediate in the oxidation of amines and sulfur compounds with hydrogen peroxide[2] or in metal-mediated oxidation reactions in biochemistry[3] and in the gas phase.[4] Several theoretical investigations[2,5] have demonstrated that water oxide rests in a flat well on the $^1[H_2,O_2]$ potential energy surface ~47 kcal/mol above the minimum for the hydrogen peroxide tautomer (Figure 1).

Although the barrier associated with 1,2-hydrogen migration to yield hydrogen peroxide amounts to only ~3 kcal/mol, experimental evidence for the existence of neutral singlet water oxide was provided recently[6] by neutralization-reionization mass spectrometry (NRMS).[7] The most conclusive experiment[6] involved sequential electron transfer to a beam of $[H_2,O_2]^{\bullet+}$ cations[8] to form the neutral species and then, with a time delay, the corresponding anion radicals.[9] Detailed analysis of the respective potential energy surfaces led to the conclusion that only the transient formation of neutral water oxide can account for the experimental findings,[6] because hydrogen peroxide cannot yield long-lived $[H_2,O_2]^{\bullet-}$ anions due to a negative electron affinity of about −58 kcal/mol.

However, a facile 1,2-hydrogen migration imparts kinetic instability to water oxide, thus preventing its isolation, not to mention bulk production, in the condensed phase, where, bimolecular hydrogen transfers may also lead to tautomerization. This kinetic instability raises the question whether derivatives

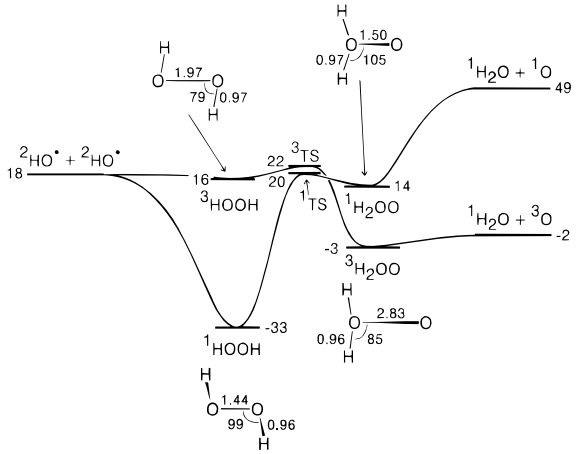

Figure 1. Calculated singlet and triplet potential energy surfaces of the $^1[H_2,O_2]$ and $^3[H_2,O_2]$ systems as adopted from ref 6. Heats of formation are given in kcal/mol.

of water oxide in which one or both hydrogen atoms are replaced by substituents with smaller migratory aptitudes would have higher kinetic stability. Dimethyl ether oxide, the parent compound of a new class of potentially stable ylides R_2O^+—O^- (R = alkyl), may be kinetically much more stable toward intra- and intermolecular rearrangements to dimethyl peroxide. If theory predicts dimethyl ether oxide and similar species to be kinetically stable, the question of their experimental generation and characterization arises. Their preparation would be quite interesting because ether oxides are expected to constitute a class of potent oxidation reagents. In addition, hydrogen abstraction

S1089-5639(97)02986-1 CCC: $15.00
Published on Web 01/16/1998

according to eq 1, which is exothermic for R−H bond energies,[10,11] below ∼115 kcal/mol for H_2OO, is expected to occur as well for R_2OO (R = H, alkyl):

$$H_2OO + R{-}H \rightarrow H_2O + OH^{\bullet} + R^{\bullet} \qquad (1)$$

Here we present a detailed theoretical investigation of neutral and ionized dimethyl ether oxide at the BECKE3LYP/6-311++G(d,p) level of theory. Some calibration calculations for the water oxide system demonstrate that the economic BECKE3LYP method is sufficiently accurate as far as geometries, energies, and vibrational frequencies are concerned. Further, methanol oxide is studied as a model in which both the 1,2-migration of hydrogen and of methyl may occur. For these systems, the energy demand for various unimolecular decomposition processes was determined to assess the kinetic stability of the ylides. One of these processes corresponds to the spin-forbidden loss of a triplet oxygen atom, for which the critical point is the minimum-energy crossing point (MECP) between the singlet and triplet potential energy surfaces. These points were also determined by a recently developed method.[12]

Computational Details

The calculations were carried out with the BECKE3LYP DFT/HF hybrid method as implemented in the Gaussian 94[13] program, using the BECKE3 parameter fit for atomization energies and the G2 set[14] for the ionization energies of small molecules. The standard triple *z* split basis set (6-311G)[15] was augmented by additional diffuse and polarization functions resulting in a 6-311++G(d,p) basis. This kind of basis set is necessary for a proper description of hydrogen shifts, loosely bound complexes[16] such as $CH_3O^{-}{\cdot}HO^{\bullet}$, and electron affinities.[17] Vibrational frequencies were calculated for each optimized structure to characterize stationary points as minima (no imaginary frequency) or transition structures (TS, one imaginary frequency) and to account for zero-point vibrational energies (ZPVE). For comparison with experimental frequencies, the calculated wavenumbers were scaled with factors of 0.96 (BECKE3LYP), 0.95 (CCSD(T)),5d, and 0.94 (MP2).[18] With few exceptions (mentioned later), the heats of formation calculated with BECKE3LYP are within ±5 kcal/mol,[19,20] of experimental data.[10] To facilitate comparison with other data, all energies are given as heats of formation in kcal/mol relative to the associated reference systems (discussed later). The $\langle S^2 \rangle$ expectation values indicating possible spin contamination were in the expected range for all calculations (i.e., ∼0.0 for singlets, 0.75 for doublets, and 2.0 for triplets). To verify some reaction pathways, the most crucial transition structures were investigated at the BECKE3LYP/6-311++G(d,p) level of theory, with the intrinsic reaction coordinate (IRC)[21] algorithm as introduced by Gonzalez and Schlegel.[22]

To evaluate the performance of the BECKE3LYP approach for the prediction of energies, geometries, and frequencies of alcohol and ether oxides, some complementary calculations for the $^1[H_2,O_2]$ system were carried out at the MP2/6-311++G(d,p) level of theory as implemented in the Gaussian 94 program package. These results were compared with earlier CCSD(T)/TZ2P+f calculations as reported by Huang et al.[5d] Further, the barrier height for the 1,2-hydrogen shift in methanol oxide was checked by G2 calculations; the latter are expected to be within an error range of ±2 kcal/mol.[14,20]

For neutral water, methanol, and dimethyl ether oxides, the corresponding triplet states are located energetically below the singlet minima. Hence, consideration of the MECPs of the singlet and triplet surfaces is indicated for the estimation of the kinetic stabilities of the singlet molecules. These MECPs were located with BECKE3LYP by method[12] that involves a geometry optimization following a composite energy gradient derived at each step from the energies and gradients of the singlet and triplet surfaces. This gradient is the sum of one term that points toward the crossing hyperline between the two surfaces and one that points toward the minimum along the hyperline. Because only small differences in energies and geometries were observed when the MECP for water oxide was located at the BECKE3LYP/6-311++G(d,p) and BECKE3LYP/6-31+G(d) levels, the smaller 6-31G(d) basis set, with 6-31+G(d) for the oxygen atoms, was used in the MECP calculations for methanol and dimethyl ether oxides.

Results and Discussion

Before discussing the theoretical results for methanol and dimethyl ether oxide systems, an evaluation of the reliability of the computational approach is indicated. For this purpose, we first describe some test calculations for the hydrogen peroxide/water oxide system. Subsequently, the theoretical predictions for methanol and dimethyl ether oxides are presented and some conceptual aspects with regard to an experimental detection of these molecules are discussed.

Test Calculations on the $^1[H_2,O_2]$ Potential Energy Surface. A series of benchmark calculations for neutral $[H_2,O_2]$ has been carried out by Schaefer and co-workers at the CCSD(T) level of theory.[5c,d] However, this level is hardly reasonable for larger systems, such as dimethyl ether oxide, because of the need for enormous computational resources that is in no sensible relation to the improvement of the accuracy. Thus, we computed neutral $[H_2,O_2]$ at the BECKE3LYP/6-311++G(d,p), MP2/6−311++G(d,p), and G2 levels of theory and compared these results with CCSD(T)/TZ2P+f data that serve as a reference.[5d]

Particular attention will be paid to the calculation of vibrational frequencies at different levels of theory,[5d,23] whereas energetic and geometric features of neutral $^1[H_2,O_2]$ have been described in detail before.[5c,9c] The computed energetics (Table 1) are quite similar for all methods, and BECKE3LYP results match quite well with those of CCSD(T) and also G2 energies, whereas MP2 slightly underestimates the stability of water oxide and the transition structure relative to hydrogen peroxide. Similarly, the computed geometries of hydrogen peroxide (Table 2) compare favorably with experimental results.[24] A minor deviation concerns a slight overestimation of the dihedral angle HOOH with BECKE3LYP and MP2 as compared with the experimental result; however, the potential for the rotation of the O−O bond is rather flat. More important, MP2 leads to a significantly shorter O−O bond for water oxide than BECKE3LYP and CCSD(T), whereas the other parameters are similar. MP2 also leads to a shorter O−O bond in the associated TS, although somewhat larger deviations of the other geometrical parameters are also found for the other two methods.

If the frequency calculations for water oxide and its higher analogues are to give meaningful results, a reasonable theoretical description of the O−O bond is mandatory. All three levels of theory examined here meet this criterion for hydrogen peroxide (i.e., the calculated frequencies are close to each other and also compare well with experimental results). For water oxide, however, the MP2 frequencies differ from those obtained with BECKE3LYP and CCSD(T) (Table 3), which in turn are similar to each other.[25,26] Recent studies on related oxygen compounds, such as carbonyl oxides and dioxiranes, have demonstrated that

TABLE 1: Calculated Total Energies (E_t, Hartree), Including Zero-Point Vibrational Energies (ZPVE) and Heats of Formation (ΔH_f, kcal/mol), of Hydrogen Peroxide, Water Oxide, and the Transition Structure for the 1,2-Hydrogen Migration Derived at Different Levels of Theory[a]

	B3LYP/6-311++G(d,p)		MP2/6-311++G(d,p)		G2		CCSD(T)/TZ2P+f[b]
species	E_t	ΔH_f	E_t	ΔH_f	E_t	ΔH_f	ΔH_f
HOOH	−151.575731	−32.6	−151.216002	−32.6	−151.362544	−32.6	−32.6
TS	−151.495738	17.6	−151.125750	23.7	−151.286485	15.1	17.5
H_2OO	−151.503372	12.8	−151.133923	18.6	−151.289595	13.2	14.2

[a] ΔH_f values are given relative to ΔH_f(HOOH) = −32.6 kcal/mol. [b] Taken from ref 5d and adopted to the ΔH_f scale.

TABLE 2: Geometries Calculated at Different Levels of Theory for the $^1[H_2,O_2]$ Isomers in Comparison to Experimental Data[a]

parameter	B3LYP/ 6-311++G(d,p)	MP2/ 6-311++G(d,p)	CCSD(T)/ TZ2P+f[b]	exptl[c]
		Water Oxide		
r(O−O)	1.553	1.498	1.549	
r(O−H)	0.970	0.969	0.967	
∠HOH	107.2	106.1	106.4	
∠oop[a]	67.7	65.6	73.4	
		Transition Structure[d]		
$r(O^1-O^2)$	1.630	1.564	1.634	
$r(H^1-O^1)$	1.044	1.021	1.031	
$r(H^1-O^2)$	1.366	1.408	1.398	
$r(H^2-O^1)$	0.970	0.970	0.968	
$\angle H^2O^1O^2$	100.1	100.2	97.4	
$\angle H^1O^1O^2H^2$	90.6	93.0	103.8	
		Hydrogen Peroxide		
r(O−O)	1.454	1.450	1.461	1.464
r(O−H)	0.967	0.965	0.964	0.965
∠HOO	100.5	99.6	99.7	99.4
∠HOOH	121.3	121.5	111.9	111.8

[a] Bond lengths are given in Å, angles in degrees. The out-of-plane angle for water oxide is defined as the angle between the O−O bond and the HOH plane. [b] Taken from ref 5d. [c] Taken from ref 24. [d] O^1 is the oxygen connected to both hydrogens; H^1 corresponds to the migrating hydrogen atom.

the CCSD(T) level of theory leads to a satisfying agreement between calculated and experimental frequencies for matrix-isolated species.[27] In fact, carbonyl oxides were known to be a notorious case for frequency calculations using almost all other computational methods, and hence we regard the CCSD(T) results as a reference for water oxide, too. For the O−O stretching mode ν_6 of water oxide, BECKE3LYP is in excellent agreement with CCSD(T) (619 versus 633 cm^{-1}), whereas MP2 is >100 wavenumbers too large (737 cm^{-1}). Similarly, the modes ν_4 and ν_5, which involve the O−O bond, are much higher with MP2 than with BECKE3LYP and CCSD(T). Hence, we assume that BECKE3LYP is more appropriate than MP2 for calculating the frequencies of higher homologues such as methanol and dimethyl ether oxides. In addition, the D- and ^{18}O-labeled systems have been calculated with BECKE3LYP (Table 4). The isotope shifts follow expectations; for example, ^{18}O labeling of water oxide to yield $H_2{}^{18}O^{16}O$ affects the O−O and O−H stretching modes ν_1, ν_2, and ν_6 by about −10 and −20 cm^{-1}, whereas ^{18}O labeling of the terminal oxygen atom, $H_2{}^{16}O^{18}O$, only leads to a shift of the O−O stretching mode ν_6 of about −15 cm^{-1}.

Besides intra- and intermolecular rearrangement to the hydrogen peroxide, a third possibility for the decay of neutral singlet water oxide exists; that spin crossing to the triplet $^3[H_2,O_2]$ potential energy surface may be followed by O−O bond cleavage (Figure 1). The triplet analogue of water oxide corresponds to a van der Waals complex of a water molecule and a triplet oxygen atom that is only weakly bound by ∼1 kcal/mol relative to the $H_2O + O(^3P)$ exit channel, but is predicted to be ∼17 kcal/mol more stable than singlet water oxide. Thus, it seems mandatory to determine the MECP between the two spin states. The MECP for water oxide is ∼5 kcal/mol above the ^1H_2OO minimum as determined with BECKE3LYP using 6-31+G(d) and 6-311++G(d,p) basis sets (Table 5). The similarities in energetics as well as in the geometric features of the MECP obtained with different basis sets suggest that the smaller basis set can safely be used in locating the MECP for the higher analogues. As to the kinetic stability of water oxide, we conclude that besides rearrangements, the singlet−triplet crossing represents a low-energy pathway for its decomposition into water and atomic oxygen.[28] From a chemical point of view, these calculations shed new light on the water oxide system in that the MECP between the singlet and triplet potential energy surfaces is energetically accessible and may compete with intramolecular rearrangement to hydrogen peroxide.

To summarize, these calibration calculations suggest that BECKE3LYP/6-311++G(d,p) is a reasonable computational level for describing the energetics, geometries, and frequencies of water oxide and its higher analogues. To further evaluate the computational performance, relevant fragments were calculated with BECKE3LYP (Table 6) and compared with literature values[10] as well as G2 computations. In general, the agreement of the BECKE3LYP results with literature data and G2 energies is good. Further, the deviations seem to scatter statistically and to not depend on the specific nature of the species described (i.e., ions or neutrals; open- or closed-shell systems). A notable exception concerns the ionization energy (IE) of dimethyl ether, which is calculated as 9.7 eV with BECKE3LYP as compared with a recommended literature value of 10.025 ± 0.025 eV.[29]

Methanol Oxide: Singlet and Triplet $[C,H_4,O_2]$ Neutrals. The two-dimensional potential energy surfaces relevant for neutral methanol oxide are depicted in Figure 2. The computed energetics (Table 7) are in reasonable agreement with literature data[10] and previous calculations.[2,30] Three crucial points (i.e., the methyl hydroperoxide, methanol oxide, and the transition structure for mutual interconversion via 1,2-hydrogen migration) have also been calculated at the G2 level of theory; G2 energies of some exit channels were taken from Curtis et al.[14a] The structures of BECKE3LYP/6-311++G(d,p)-optimized $^1[C,H_4,O_2]$ isomers and transition states connecting them are shown in Chart 1.

Both singlets, methyl hydroperoxide **^{1}1** and methanol oxide **^{1}2**, represent local minima on the $^1[C,H_4,O_2]$ potential energy surface (Figure 2), and BECKE3LYP predicts the hydroperoxide to be more stable by 56 kcal/mol. Considering a stability difference of 45 kcal/mol between hydrogen peroxide and water oxide, the gap between **^{1}1** and **^{1}2** may be somewhat overestimated. Indeed, G2 calculations (Table 7) predict a heat of formation for methyl hydroperoxide that is ∼5 kcal/mol higher (ΔH_f = −32.6 instead of −37.2 kcal/mol) than the BECKE3LYP value, whereas methanol oxide is lower in energy with G2 by ∼7 kcal/mol (ΔH_f = 11.1 instead of 18.5 kcal/mol). Conse-

TABLE 3: Calculated Frequencies (cm^{-1}) and Intensities (in brackets, km/mol) of $^1[H_2,O_2]$ Isomers at Different Levels of Theory[a]

parameter	B3LYP/6-311++G(d,p)	MP2/6-311++G(d,p)	CCSD(T)/TZ2P+f[b]	exptl[c]
		Water Oxide		
ν_1 OH sym str	3656 (185)	3620 (187)	3648 (177)	
ν_2 OH asym str	3564 (80)	3517 (91)	3554 (68)	
ν_3 HOH bend	1522 (93)	1498 (79)	1545 (91)	
ν_4 OOH asym bend	852 (2)	893 (3)	806 (<1)	
ν_5 out of plane	820 (103)	916 (97)	836 (89)	
ν_6 O—O str	619 (93)	737 (90)	633 (113)	
		Transition Structure		
ν_1 OH str	3615 (120)	3569 (149)	3598 (112)	
ν_2 OH str	2762 (116)	2986 (133)	2851 (91)	
ν_3 out of plane	1310 (109)	1331 (107)	1378 (89)	
ν_4 OOH bend	926 (52)	l952 (30)	879 (66)	
ν_5 O—O str	620 (39)	755 (35)	637 (23)	
ν_6 reaction coordinate	1127i	1214i	1048i	
		Hydrogen Peroxide		
ν_1 OH sym str	3613 (13)	3605 (16)	3613 (13)	3607
ν_2 OH asym str	3613 (68)	3605 (71)	3611 (50)	3608
ν_3 OOH sym bend	1389 (<1)	1363 (<1)	1355 (<1)	1393
ν_4 OOH asym bend	1238 (92)	1216 (102)	1256 (102)	1266
ν_5 O—O str	846 (1)	817 (1)	846 (1)	863
ν_6 torsion	350 (228)	369 (228)	372 (166)	317

[a] The frequencies have been scaled by 0.96 for BECKE3LYP, 0.94 for MP2, and 0.95 for CCSD(T), see ref 18. [b] Taken from ref 5d. [c] Taken from Giguere, P. A.; Srinivasan, T. K. K. *J. Raman Spectrosc.* **1974**, *2*, 125.

TABLE 4: Frequency Shifts for ^{2}H- and ^{18}O-Labeled Isotopologues of Water Oxide and Hydrogen Peroxide Calculated at the Becke3LYP/6-311++G(d,p) Level of Theory for Water Oxide and Hydrogen Peroxide

	H_2OO*a*	$H_2{}^{18}OO$	$H_2O^{18}O$	$H_2{}^{18}O^{18}O$	D_2OO*a*	$D_2{}^{18}OO$	$D_2O^{18}O$	$D_2{}^{18}O^{18}O$	HOOH[a]	$H^{18}OOH$	$H^{18}O^{18}OH$	DOOD[a]	$D^{18}OOD$	$D^{18}O^{18}OD$
parameter	ν (cm^{-1})	$\Delta\nu$ (cm^{-1})	$\Delta\nu$ (cm^{-1})	$\Delta\nu$ (cm^{-1})	ν (cm^{-1})	$\Delta\nu$ (cm^{-1})	$\Delta\nu$ (cm^{-1})	$\Delta\nu$ (cm^{-1})	ν (cm^{-1})	$\Delta\nu$ (cm^{-1})	$\Delta\nu$ (cm^{-1})	ν (cm^{-1})	$\Delta\nu$ (cm^{-1})	$\Delta\nu$ (cm^{-1})
ν_1 OH sym str	3656	−18	−1	−18	2684	−23	0	−23	3613	0	−13	2644	−2	−18
ν_2 OH asym str	3564	−9	−2	−9	2566	−11	0	−11	3613	−12	−12	2640	−16	−18
ν_3 HOH bend	1522	−5	1	−5	1111	−7	0	−7	1389	−4	−7	1025	−4	−9
ν_4 OOH asym bend	852	−2	−5	−8	706	−6	−17	−22	1238	−4	−7	918	−3	−8
ν_5 out of plane	820	−2	−1	−3	601	−2	−2	−4	846	−26	−53	895	−28	−53
ν_6 OO str	619	−18	−15	−35	581	−16	−5	−22	350	−2	−3	257	−1	−2

[a] The frequencies are scaled by a factor of 0.96 (ref 18).

TABLE 5: Calculated O—O Bond Lengths (Å) and Relative Energies (kcal/mol) as Derived from MECP Calculations for Water-, Methanol-, and Dimethyl Ether Oxides at the Becke3LYP Level of Theory[a]

		singlet minimum		MECP		$H_2O + O(^3P)$
oxide	basis set	r(OO)	E_{rel}[b,c]	r(OO)	E_{rel}[b]	E_{rel}[b]
H_2OO	6-311++G(d,p)	1.553	0.0	1.772	5.0	−11.8
	6-31G(d)[d]	1.548	0.0	1.776	6.0	−8.8
$CH_3(H)OO$	6-311++G(d,p)	1.511	0.0			−3.0
	6-31G(d)[d]	1.510	0.0	1.795	10.0	−0.3
$(CH_3)_2OO$	6-311++G(d,p)	1.489	0.0			−2.0
	6-31G(d)[d]	1.488	0.0	1.824	13.6	−4.3

[a] The complete geometrical data for these MECPs are given in the Appendix. [b] Zero-point vibrational energy corrections have not been considered for the relative energies given here. [c] The energy of the singlet minimum was chosen as reference point. [d] The 6-31G(d) basis was applied for all except the two oxygen atoms (6-31+G(d)).

quently, the energy gap between **^{1}1** and **^{1}2** is only 44 kcal/mol at the G2 level, which is quite similar to that found for the hydrogen peroxide/water oxide system.

With respect to the calculated frequencies (Table 8), neutral methanol oxide exhibits features similar to water oxide for the OH (ν_1, 3596 cm^{-1}) and OO (ν_{13}, 658 cm^{-1}) stretching and OOH bending modes (ν_{12}, 835 cm^{-1}), which can be clearly identified by their isotopic shifts upon ^{18}O incorporation. The OO-stretching does not shift upon deuteration, whereas the OOH bending mode decreases from 835 to 583 cm^{-1} for OOD. The CO stretching mode (ν_9) is found in the usual region[31] at 1133 cm^{-1} and is influenced only by ^{18}O labeling of the participating oxygen atom. The COH and COO bending vibrations (ν_{11}, ν_{14}) are predicted as 920 cm^{-1} and 343 cm^{-1}, respectively, with corresponding isotopic shifts. Further, the CH stretching (ν_2—ν_4) and CH deformation modes (ν_5—ν_7) are hardly affected by ^{18}O labeling; of course, these modes shift largely when hydrogen is replaced by deuterium. Probably because of the particular bonding situation in the ylide, the CH stretching modes appear at somewhat larger wavenumbers (>3000 cm^{-1}) than usually.[36]

Three barriers associated with different types of isomerization processes connect **^{1}1** and **^{1}2**. The transition structure **^{1}TS1/2-H** for 1,2-hydrogen migration from one oxygen to the other, lies 5.1 kcal/mol above methanol oxide as determined with BECKE3LYP/6-311++G(d,p). This barrier height is in good agreement with the value of 4.9 kcal/mol obtained from G2 calculations. So far, the $^1[C,H_4,O_2]$ system resembles much that of water oxide (Figure 1). However, two additional transition structures have been located that are associated with 1,2-methyl migrations.[32] The first, **^{1}TS1/2-CH$_3$**, describes a methyl shift that proceeds with retention of configuration at the migrating carbon atom. This TS is higher in energy than **^{1}2** by ~35 kcal/mol. The second one, **^{1}TS1/2-CH$_3$′** involves a methyl shift with inversion of configuration and is 41 kcal/mol higher in energy than **^{1}2**. In fact, these barriers for methyl shifts are higher in

TABLE 6: Calculated Total Energies (E_t), Zero-Point Vibrational Energies (ZPVE), and Experimental and Calculated Heats of Formation (ΔH_f) of Fragmentation Products

fragmentation product	E_t(B3LYP)[a] (Hartree)	ZPVE (Hartree)	E_t(G2)[b] (Hartree)	ΔH_f (lit)[c] (kcal/mol)	ΔH_f(B3LYP)[d] (kcal/mol)	ΔH_f(G2)[d] (kcal/mol)
$H^\bullet$	−0.502257		−0.50000	52.1		
^3O	−75.089880		−74.98203	59.6		
$O^{\bullet-}$	−75.149014		−75.03341	25.9	22.5	27.4
$OH^\bullet$	−75.753967	0.008445	−75.64391	9.3		
$^3OH^+$	−75.268751	0.006971	−75.16702	309.3	313.8	308.6
OH^-	−75.818918	0.008530	−75.71276	−32.8	−31.5	−33.9
$CH_3^\bullet$	−39.825553	0.029635	−39.74509	34.8		
CH_3^+	−39.460306	0.031166	−39.38274	261.7	264.0	262.2
$HOO^\bullet$	−150.943996	0.014067	−150.72773	2.5		
$1HOO^+$	−150.497979	0.013944			282.4	
$^3HOO^+$	−150.522540	0.012937		264.2	267.0	
HOO^-	−150.982563	0.012912		−22.3	−21.7	
$CH_3O^\bullet$	−115.056175	0.036069		3.7		
$3CH3O^+$	−114.667039	0.033136		247.4[e]	247.9	
CH_3O^-	−115.112312	0.034502		−32.5	−31.5	
$CH_2OH^\bullet$	−115.065474	0.037061	−114.88155	−6.2		
CH_2OH^+	−114.781609	0.040477		168.1	171.9	
CH_3OH	−115.713972	0.051026	−115.53489	−48.2		
$CH_3OH^{\bullet+}$	−115.324472	0.046997		201.3	196.2	
$CH_3OO^\bullet$	−190.235866	0.042718	−189.94303	2.4[f]		
$^1CH_3OO^+$	−189.839746	0.042026		247.5[f]	251.0	
$^3CH_3OO^+$	−189.858528	0.041306		240.1[f]	239.2	
CH_2OOH^+	−189.932174	0.043714		188.3[g]	193.0	
CH_3OO^-	−190.277534	0.040806			−23.7	
$CH_3OCH_2^\bullet$	−154.349568	0.065346		−2.8		
$CH_3OCH_2^+$	−154.087761	0.068432		157.2	161.5	
CH_3OCH_3	−154.997882	0.079232		−44.0		
$CH_3OCH_3^{\bullet+}$	−154.642798	0.075660		187.2	178.8	
$CH_3OOCH_2^+$	−229.236097	0.070934				

[a] Total energies include unscaled ZPVE corrections. [b] Total energies based on G2 calculations; some of these energies were taken from ref 14. [c] Taken from ref 10. [d] Heats of formation of ionic species were calculated from the difference of total energies of ionic and neutral molecules of the same elemental composition taking the literature data for the corresponding neutral(s) as a reference. [e] Fergusson, G. G.; Roncin, J. L. *Int. J. Mass Spectrom. Ion Processes* **1987**, *79*, 215. [f] Cheung, Y.-S.; Li, W.-K. *Chem. Phys. Lett.* **1994**, *223*, 383; ibid, *J. Mol. Struct. (Theochem.)* **1995**, *333*, 135. [g] Holmes, J. L.; Mommers, A. A.; de Koster, C.; Herrma, W.; Terlouw, J. K. *Chem. Phys. Lett.* **1985**, *115*, 439.

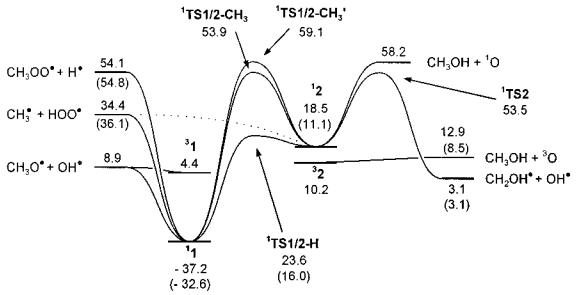

Figure 2. Calculated singlet and triplet potential energy surfaces of the $^1[C,H_4,O_2]$ and $^3[C,H_4,O_2]$ systems at the BECKE3LYP/6-311++G(d,p) level of theory. G2 energies are given in brackets.

energy than the $HOO^\bullet + CH_3^\bullet$ exit channel (Figure 2), which causes some doubts as to whether these transition structures are real. To this end, IRC calculations were performed to follow the reaction path downhill. These calculations demonstrate that the two transition structures indeed connect the minima for **^{1}1** and **^{1}2** (Figure 3). With respect to the geometries of the three transition structures, the O−O bond lengths (Chart 1) exhibit a rather unconventional behavior. Upon isomerization from **^{1}1** to **^{1}2** via **^{1}TS1/2-H**, the O−O bond increases from 1.460 Å for **^{1}1** to 1.598 Å in the transition structure and reaches 1.511 Å in **^{1}2**. Similarly, upon methyl shift under retention of configuration, the O−O bond is longer in **^{1}TS1/2-CH$_3$** (1.541 Å) than in the two minima. This result is quite usual for three-membered transition structures and was also found for the 1,2-hydrogen migration in water oxide.[5,6] However, if the methyl group is shifted with inversion of configuration, the O−O bond drastically shortens in **^{1}TS1/2-CH$_3$′** (1.361 Å) to a value close to that of the $HOO^\bullet$ radical (r(O−O) = 1.328 Å at the same level of theory). Together with the rather long C−O bond distances in **^{1}TS1/2-CH$_3$′** (2.538 and 2.396 Å), this result points to a methyl radical migrating between the two oxygen atoms of a $HOO^\bullet$ radical with only a very small orbital interaction. Hence, the electron−electron repulsion of the two oxygen atoms is reduced compared with the minima, and the O−O bond becomes shorter. Nevertheless, in summary, both methyl transfers are much too energy demanding and cannot compete with the 1,2-H shift. The barrier for hydrogen migration is very low, as already found for water oxide, so that the bulk generation of alcohol oxides appears impossible. However, one may expect that substitution of both hydrogens in H_2O_2 by methyl groups may lead to a significant kinetic stabilization of the corresponding ether oxide.

The lowest exit channel for **^{1}1** corresponds to O−O bond cleavage to yield $OH^\bullet$ and $CH_3O^\bullet$ radicals and requires 46 kcal/mol, which is consistent with an experimental bond dissociation energy[10] of 44 kcal/mol and a G2 value of 45 kcal/mol.[33] Rearrangement to methanol oxide via 1,2-H shift is of comparable energy demand, but entropically disfavored. With respect to the methanol oxide minimum, the 1,2-H migration (5.1 kcal/mol) concomitant with subsequent O−O bond cleavage represents the reaction pathway of lowest energy demand, followed by the $CH_3^\bullet + HOO^\bullet$ exit channel located 16 kcal/mol above **^{1}2**. In addition, a transition structure, **^{1}TS2**, was found 35 kcal/mol above **^{1}2**, which describes the dissociation of methanol oxide into $OH^\bullet$ and $CH_2OH^\bullet$ via formal 1,2-elimination.

On the triplet surface of $[C,H_4,O_2]$ (Figure 2), two isomers, **^{3}1** and **^{3}2** were located. The structures of **^{3}1** and **^{3}2** are best

TABLE 7: Calculated Total Energies (E_t), Zero-Point Vibrational Energies (ZPVE), and Calculated and Experimental Heats of Formation (ΔH_f) of Singlet and Triplet [C,H$_4$,O$_2$] Isomers and Relevant Fragmentation Reactions

isomer/fragment	E_t(B3LYP)[a] (Hartree)	ZPVE (Hartree)	E_t(G2)[b] (Hartree)	ΔH_f(B3LYP)[c] (kcal/mol)	ΔHf(G2)[c] (kcal/mol)	ΔH_f[d] (kcal/mol)
^{1}CH$_3$OOH ^{1}1	−190.864851	0.054360	−190.58238	−37.2	−32.6	−31.3
^{1}CH$_3$(H)OO ^{1}2	−190.794858	0.055219	−190.51264	18.5	11.1	
^{1}TS1/2-H	−190.785830	0.050488	−190.50496	23.6	16.0	
^{1}TS1/2-CH$_3$	−190.738531	0.051880		53.9		
^{1}TS1/2-CH$_3$′	−190.730255	0.050193		59.1		
^{1}TS2	−190.739108	0.048649		53.5		
^{3}CH$_3$OOH ^{3}1	−190.815806	0.048489		4.4		
^{3}CH$_3$(H)OO ^{3}2	−190.808087	0.051888		10.2		
CH$_2$OH$^\bullet$ + OH$^\bullet$	−190.819441	0.045506	−190.52546	3.1	3.1	3.1
CH$_3$O$^\bullet$ + OH$^\bullet$	−190.810142	0.044514		8.9		13.0
CH$_3$OH + ^{3}O	−190.803852	0.051026	−190.51692	12.9	8.5	11.4
CH$_3^\bullet$ + HOO$^\bullet$	−190.769549	0.043702	−190.47282	34.4	36.1	37.3
CH$_3$OO$^\bullet$ + H$^\bullet$	−190.738123	0.042718	−190.44303	54.1	54.8	54.5
CH$_3$OH + ^{1}O[e]				58.2		56.7
CH$_2$OH$^+$ + OH$^-$	−190.600527	0.049007		140.5		135.3

[a] Total energies based on Becke3LYP/6-311++G(d,p)-optimized structures including unscaledZPVE corrections. [b] Total energies based on G2 calculations; some of these energies were taken from ref 14a. [c] Calculated on the basis of literature data for the CH$_2$OH$^\bullet$ + OH$^\bullet$ exit channel. [d] Experimental reference data as given in Table 6 and ref 10. [e] Because BECKE3LYP calculations are problematic with the excited singlet state of oxygen atoms, the excitation energy of 1.967 eV relative to the triplet ground state has been added to the calculated energy for the triplet species for data, see Herzberg, G. *Electronic Spectra and Electronic Structure of Polyatomic Molecules*; Van Nostrand: Princeton, NJ, 1966.

CHART 1

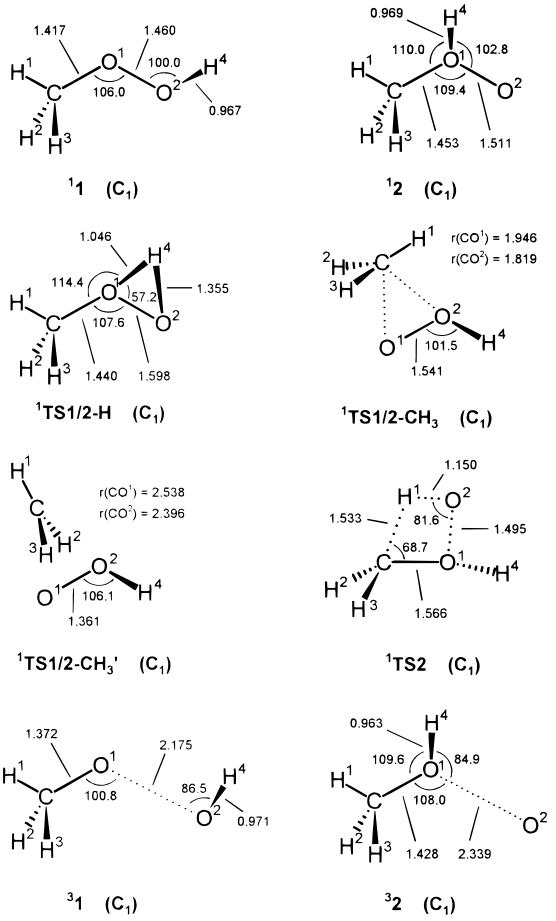

described as weakly bound ^{3}[CH$_3$O···OH] and [CH$_3$OH·^{3}O] van der Waals complexes with large O−O distances of 2.175 and 2.339 Å, respectively, and low dissociation energies of 4.5 and 2.7 kcal/mol into CH$_3$O$^\bullet$ + $^\bullet$OH or CH$_3$OH + O (^{3}P), respectively. As on the ^{3}[H$_2$O$_2$] surface, triplet methanol oxide is lower in energy than its singlet analogue by ˜9 kcal/mol, such that low-lying crossing points between the singlet and triplet surfaces may contribute to the reactivity of methanol oxide. The corresponding MECP was located at a geometry very similar to that of methanol oxide, but with the O−O bond elongated to 1.795 Å (Table 5) and an energy demand of ∼10 kcal/mol relative to **^{1}2**. Thus, the MECP is predicted to be higher than the barrier for the 1,2-hydrogen migration by ∼5 kcal/mol, and although the spin crossover may play a role for water oxide, it is expected to be negligible for the reactivity of singlet methanol oxide.

In conclusion, neutral methanol oxide is predicted to be a stable molecule, although it is expected to be at least as hard to identify and characterize by experimental means as water oxide[6] due to the extremely low kinetic stabilization against 1,2-hydrogen migration.

The ^{2}[C,H$_4$,O$_2$]$^{\bullet+}$ Cation. A different picture evolves from the calculated cationic ^{2}[C,H$_4$,O$_2$]$^{\bullet+}$ potential energy surface (Figure 4). For both isomeric cation radicals, ionized methyl hydroperoxide **1**$^{\bullet+}$ and ionized methanol oxide **2**$^{\bullet+}$, distinct minima exist. The energy difference between these two entities amounts to 24 kcal/mol (Table 9), which is much lower than the gap between the two neutral tautomers of ∼45 kcal/mol. Similar situations were encountered for water oxide and several other ylides, such as CH$_2$OH$_2$, CH$_2$ClH, and CH$_2$NH$_3$ and their cationic counterparts.[5b,8b,34] For example, the conventional CH$_3$OH isomer is much more favorable in energy than the ylide structure CH$_2$OH$_2$ due to the formal charge separation in the ylide, whereas the α-distonic[35] ylide cation-radical $^\bullet$CH$_2$OH$_2^+$ is actually more stable than its conventional isomer CH$_3$OH$^{\bullet+}$.[36] Moreover and also in analogy to other distonic ions, **1**$^{\bullet+}$ and **2**$^{\bullet+}$ are separated by significant barriers. Again, one transition structure, **TS1/2-H**$^{\bullet+}$, could be located for the 1,2-hydrogen shift, but for the cationic species, this barrier is quite high. Instead, the isomerization **1**$^{\bullet+}$ → **2**$^{\bullet+}$ may proceed via two transition structures with similar energy demands involving either retention (**TS1/2-CH$_3$**$^{\bullet+}$) or inversion (**TS1/2-CH$_3$′**$^{\bullet+}$) of configuration at the carbon atom. **TS1/2-CH$_3$**$^{\bullet+}$ is located ∼25 kcal/mol above **2**$^{\bullet+}$ and represents the most favorable pathway for the rearrangement **1**$^{\bullet+}$ → **2**$^{\bullet+}$.

As far as the geometries (Chart 2) of these structures are concerned, three aspects should be briefly addressed. (i) Due to the lower amount of electron−electron repulsion between the lone pairs at the oxygen atoms, the O−O bond lengths (1.324 Å for **1**$^{\bullet+}$, 1.333 Å for **2**$^{\bullet+}$) are shorter compared with the neutral species (1.460 Å for **^{1}1**, 1.511 Å for **^{1}2**). This result is in line

TABLE 8: Calculated Frequencies for Methanol Oxide and Frequency Shifts for ^{2}H- and ^{18}O-Labeled Isotopologues Calculated at the Becke3LYP/6-311++G(d,p) Level of Theory

	$CH_3(H)OO$		$CH_3(H)^{18}OO$	$CH_3(H)^{18}O$	$CH_3(H)^{18}O^{18}O$	$CD_3(D)OO$	$CD_3(D)^{18}OO$	$CD_3(D)O^{18}O$	$CD_3(D)^{18}O^{18}O$
isotopologue	ν (cm^{-1})[a]	Int. (km/mol)	$\Delta\nu$ (cm^{-1})	$\Delta\nu$ (cm^{-1})	$\Delta\nu$ (cm^{-1})	ν (cm^{-1})[a]	$\Delta\nu$ (cm^{-1})	$\Delta\nu$ (cm^{-1})	$\Delta\nu$ (cm^{-1})
ν_1 OH str	3596	(123)	−12	0	−13	2622	−18	0	−18
ν_2 CH str	3062	(2)	0	0	0	2274	0	0	0
ν_3 CH str	3021	(8)	0	0	0	2244	0	0	0
ν_4 CH str	2930	(26)	0	0	0	2098	0	0	0
ν_5 CH def	1437	(11)	0	0	0	1034	0	0	0
ν_6 CH def	1401	(12)	−1	0	−1	1014	−1	0	−1
ν_7 CH def	1394	(0)	−1	0	−1	1068	0	0	0
ν_8	1270	(18)	−5	0	−5	982	−8	0	−8
ν_9 CO str	1133	(5)	−5	0	−5	922	−19	0	−19
ν_{10}	1050	(35)	−3	−1	−4	768	−2	−5	−6
ν_{11} COH bend	920	(26)	−21	0	−21	868	−19	−1	−18
ν_{12} OOH bend	835	(71)	−6	−5	−11	583	−8	−4	−13
ν_{13} OO str	658	(42)	−16	−17	−34	672	−6	−15	−21
ν_{14} out of plane	343	(15)	−5	−7	−12	315	−4	−7	−11
ν_{15}	218	(3)	−1	−1	−2	163	−1	−1	−2

[a] Frequencies are scaled by a factor of 0.96; see ref 18.

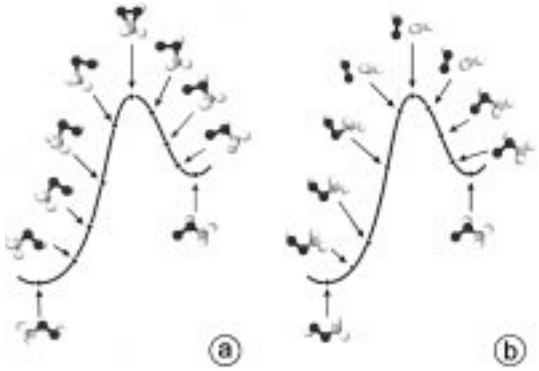

Figure 3. Snapshots from IRC calculations for **1TS1/2-CH$_3$** and **1TS1/2-CH$_3$′** representing the 1,2-methyl migrations in the neutral singlet methyl hydroperoxide/methanol oxide system with (a) retention and (b) inversion of configuration at the migrating carbon atom.

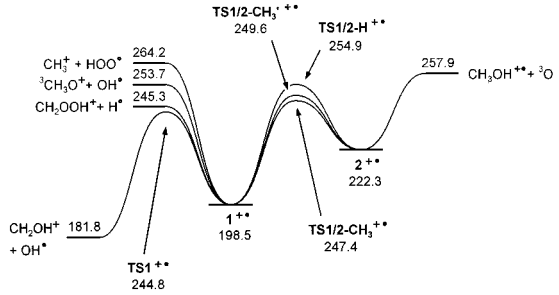

Figure 4. Calculated doublet potential energy surface of the $^2[C,H_4,O_2]^{\bullet+}$ system at the BECKE3LYP/6-311++G(d,p) level of theory.

with an increased strength of the peroxidic O−O bond in **1**$^{\bullet+}$ (55 kcal/mol) compared with that in **^{1}1** (46 kcal/mol),[31,37] which is expressed not only in a shorter O−O bond, but also in the shift of the O−O stretching frequency from 658 cm^{-1} for neutral **^{1}1** to 1015 cm^{-1} for the cation radical **1**$^{\bullet+}$. (ii) Although the ∠COOH dihedral angle in neutral methyl hydroperoxide (134.6°) is similar to the ∠HOOH angle in hydrogen peroxide (121.3°), it amounts to almost 180° for the cation. A similar effect has already been calculated for the hydrogen peroxide[6,8c,d] and dimethyl peroxide cation radicals.[42] The planarity of the COOH moiety indicates that the radical electron at one oxygen atom is delocalized with a lone pair from the other in a three-electron-two-center bond. In analogy to ionized hydrogen peroxide[8c,d] and dimethyl peroxide,[42] a cisoid structure is also expected to exist for the methyl hydroperoxide cation radical.

TABLE 9: Calculated Total Energies (E_t), Zero-Point Vibrational Energies (ZPVE), and Calculated and Experimental Heats of Formation (ΔH_f) of Doublet $[C,H_4,O_2]^{\bullet+}$ Isomers and Some Relevant Fragmentation Channels

isomer/fragment	E_t[a] (Hartree)	ZPVE (Hartree)	ΔH_f[b] (kcal/mol)	ΔH_f[c] (kcal/mol)
$CH_3OOH^{\bullet+}$ 1$^{\bullet+}$	−190.509012	0.054297	198.5	204.0[d]
$CH_3(H)OO^{\bullet+}$ 2$^{\bullet+}$	−190.471084	0.053875	222.3	
TS1/2-H$^{\bullet+}$	−190.419120	0.048162	254.9	
TS1/2-CH3$^{\bullet+}$	−190.431035	0.049498	247.4	
TS1/2-CH3′$^{\bullet+}$	−190.427636	0.048138	249.6	
TS1$^{\bullet+}$	−190.435206	0.045892	244.8	
$CH_2OH^+ + OH^\bullet$	−190.535576	0.048922	181.8	177.4
$CH_2OOH^+ + H^\bullet$	−190.434431	0.043714	245.3	240.4
$^3CH_3O^+ + OH^\bullet$	−190.421006	0.041581	253.7	256.7
$CH_3OH^{\bullet+} + 3O$	−190.414352	0.046997	257.9	260.9
$CH_3^+ + HOO^\bullet$	−190.404302	0.045233	264.2	264.2
$^3CH_3OO^+ + H^\bullet$	−190.360785	0.041306	291.5	292.2
$^3HOO^+ + CH_3^\bullet$	−190.348093	0.042572	299.5	299.0
$^1CH_3OO^+ + H^\bullet$	−190.342003	0.042026	303.3	299.6
$^3OH^+ + CH_3O^\bullet$	−190.324926	0.043040	314.0	313.0
$^1HOO^+ + CH_3^\bullet$	−190.323532	0.043579	314.9	

[a] Total energies based on BECKE3LYP/6-311++G(d,p)-optimized structures including unscaled ZPVE corrections. [b] Calculated on the basis of literature data for the $CH_3^+ + HOO^\bullet$ exit channel. [c] Experimental reference data as given in Table 6 and ref 10. [d] Estimated value with an uncertainty of ±7 kcal/mol; see Fergusson, E. E.; Roncin, J.; Bonazzola, L. *Int. J. Mass Spectrom. Ion Processes* **1987**, *79*, 215.

However, we did not pursue this subject further and regard the transoid geometry as representative for the methyl hydroperoxide cation radical. (iii) The alternation of the O−O bond lengths in the three transition structures (see previous discussion) is again found for the cationic system. The O−O bond length is increased for **TS1/2-H**$^{\bullet+}$ and **TS1/2-CH$_3$**$^{\bullet+}$ and decreased for **TS1/2-CH$_3$′**$^{\bullet+}$ compared with the two minima. However, due to the lower amount of electron−electron repulsion, this effect is less pronounced for the cation radicals.

With respect to the unimolecular reactivity of the two $[C,H_4,O_2]^{\bullet+}$ isomers, several chemically feasible exit channels were sought. The fragmentation of lowest energy demand for **2**$^{\bullet+}$ corresponds to the loss of a triplet O (^{3}P) atom yielding ionized methanol. This exit channel is, however, 10 kcal/mol higher in energy than **TS1/2-CH$_3$**$^{\bullet+}$, and although the bond cleavage is favored above rearrangement due to entropic effects, it is expected to compete inefficiently with the isomerization **2**$^{\bullet+}$ → **1**$^{\bullet+}$. In the case of **1**$^{\bullet+}$, there are two reaction pathways that lie below the barriers for rearrangement. The calculations

CHART 2

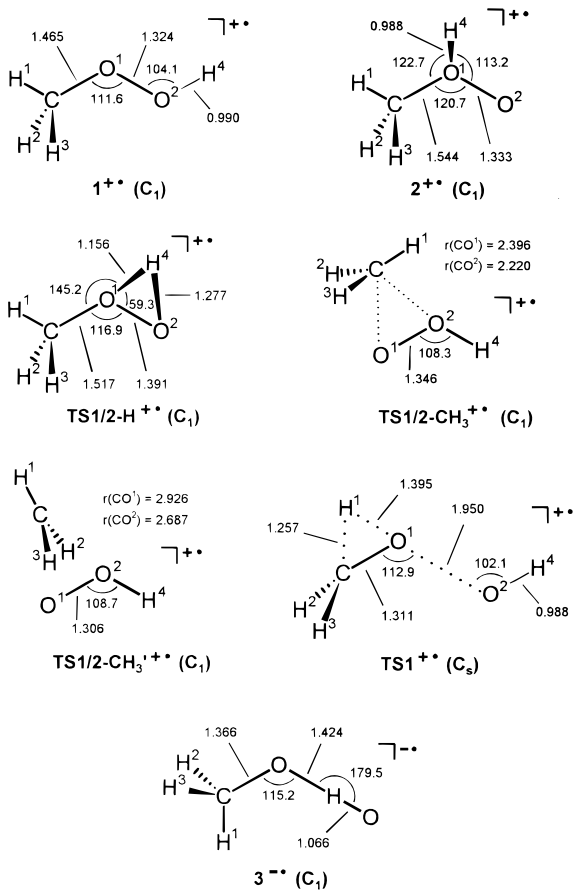

predict C−H bond cleavage as a low-lying exit channel and, indeed, loss of atomic hydrogen contributes significantly to the unimolecular chemistry[38] of metastable $\mathbf{1}^{\bullet+}$. In addition, a transition structure $\mathbf{TS1}^{\bullet+}$ was located that describes loss of an OH• radical concomitant with formation of CH_2OH^+.[39] In this process, one of the carbon-bound hydrogen atoms undergoes a 1,2-migration to the first oxygen, whereas the O−O bond is elongated. This reaction is of approximately the same energy demand as the loss of a hydrogen atom. Consistent with the fact that direct bond cleavage is entropically favored, the rearrangement accompanied by OH• loss is indeed a minor route in the unimolecular decomposition of $\mathbf{1}^{\bullet+}$. It should be noted that extensive calculations for ionized dimethyl peroxide[42] and a mass spectrometric study on larger dialkylperoxides[40] demonstrated that complex reaction paths are typical for seemingly direct losses of RO• radicals from ionized peroxides involving hydrogen-bridged ions as well as ion/dipole complexes.,[41,42] Similarly, the loss of an OH• radical from $\mathbf{1}^{\bullet+}$ is likely to proceed via hydrogen-bridged ions like, for example, $[CH_2O{-}H{-}OH]^{\bullet+}$. As this aspect has already been discussed in detail for the higher homologue,[42] it will not be pursued further here. Finally, direct O−O bond cleavage would provide a second route for the formation of OH• radicals, but is rather unlikely to occur because of the necessity of forming an energetically unfavorable triplet methoxy cation.[43]

In conclusion, the calculated $^2[C,H_4,O_2]^{\bullet+}$ potential energy surface is in good agreement with previous experimental data.[45] Unfortunately, the same experimental approach as used for the generation of neutral water oxide via the corresponding cation radical[6] cannot be applied to methanol oxide, because the isomerization $\mathbf{1}^{\bullet+} \rightarrow \mathbf{2}^{\bullet+}$ is rather unlikely to occur because of more favorable direct fragmentation channels of energized $\mathbf{1}^{\bullet+}$.

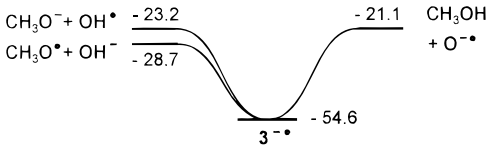

Figure 5. Calculated doublet potential energy surface of the $^2[C,H_4,O_2]^{\bullet-}$ system at the BECKE3LYP/6-311++G(d,p) level of theory.

TABLE 10: Calculated Total Energies (E_t), Zero-point Vibrational Energies (ZPVE), and Calculated and Experimental Heats of Formation (ΔH_f) of Doublet $[C,H_4,O_2]^{\bullet-}$ and Fragmentation Reactions

doublet/fragment	E_t[a] (Hartree)	ZPVE (Hartree)	ΔH_f[b] (kcal/mol)	ΔH_f[c] (kcal/mol)
$\mathbf{CH_3O^- \bullet HO^\bullet\ 3^{\bullet-}}$	−190.916341	0.045938	−54.6	
$CH_3O^\bullet + OH^-$	−190.875093	0.044599	−28.7	−29.1
$CH_3O^- + OH^\bullet$	−190.866279	0.042947	−23.2	−23.2
$CH_3OH + O^{\bullet-}$	−190.862986	0.051026	−21.1	−22.3
$HOO^- + CH_3^\bullet$	−190.808116	0.042547	13.3	12.5
$CH_3OO^- + H^\bullet$	−190.779791	0.040806	31.1	

[a] Total energies based on Becke3LYP/6-311++G(d,p)-optimized structures including unscaled ZPVE corrections. [b] Calculated on the basis of literature data for the CH_3O^- + OH• exit channel. [c] Experimental reference data as given in Table 6 and ref 10.

The $^2[C,H_4,O_2]^{\bullet-}$ Anion. Because the existence of an anion radical was a key issue in the experimental identification of neutral water oxide,[6] the discussion of methanol oxide would be incomplete without a brief comment on the $^2[C,H_4,O_2]^{\bullet-}$ potential energy surface (Figure 5, Table 10). Although on the $^2[H_2,O_2]^{\bullet-}$ surface[9c] two isomers exist (i.e., the hydrogen-bridged complexes $^2[HO^-{\cdot}HO^\bullet]$ and $^2[O^{\bullet-}{\cdot}HOH]$), only a single isomer was found for the $^2[C,H_4,O_2]^{\bullet-}$ system. The anion radical $\mathbf{3}^{\bullet-}$ (Chart 2) can be regarded as an ion/dipole complex with a resonating charge-transfer bond. It can be described with the negative charge either on the hydroxy or on the methoxy subunit (i.e., $^2[CH_3O^\bullet{\cdot}HO^-]$ or $^2[CH_3O^-{\cdot}HO^\bullet]$). All attempts to locate the isomeric $^2[CH_3OH{\cdot}O]^{\bullet-}$ form failed and optimization always led to $\mathbf{3}^{\bullet-}$.

With regard to the question of experimental characterization of methanol oxide by NRMS, the vertical electron affinities of neutral $^1\mathbf{1}$ and $^1\mathbf{2}$ are of interest; these affinities turn out to be slightly negative, with −14 kcal/mol for $^1\mathbf{1}$ and −6 kcal/mol for $^1\mathbf{2}$. A negative electron affinity means that no stable anions exist at the corresponding structures. However, as demonstrated earlier for neutral water oxide,[6] the neutrals may adopt geometries in which the electron affinities become positive. As the electron affinities at the equilibrium geometries of $^1\mathbf{1}$ and $^1\mathbf{2}$ are of the same order of magnitude − the difference was much larger for HOOH (−58 kcal/mol) versus H_2OO (−6 kcal/mol) − this may also hold true not only for methanol oxide but also for methyl hydroperoxide. Therefore, the formation of a stable $^2[C,H_4,O_2]^{\bullet-}$ anion from neutral $[C,H_4,O_2]$ via vertical electron transfer cannot be considered as unequivocal evidence for the presence of transient methanol oxide as the neutral precursor.

The $[C_2,H_6,O_2]$ Neutral. The singlet and triplet potential energy surfaces of neutral $[C_2,H_6,O_2]$ (Figure 6) are qualitatively very similar to the methanol oxide case with the exception that the 1,2-hydrogen migration is no longer possible. Two minimum structures (Chart 3) were located (i.e., dimethyl peroxide $^1\mathbf{4}$ and dimethyl ether oxide $^1\mathbf{5}$, which differ in energy by 51 kcal/mol; Table 11). With respect to the geometry of $^1\mathbf{4}$, it should be noted that the ∠COOC dihedral angle of 180° suggests a transoid structure, which is in accord with several earlier theoretical[44] and experimental[45] studies. However, due

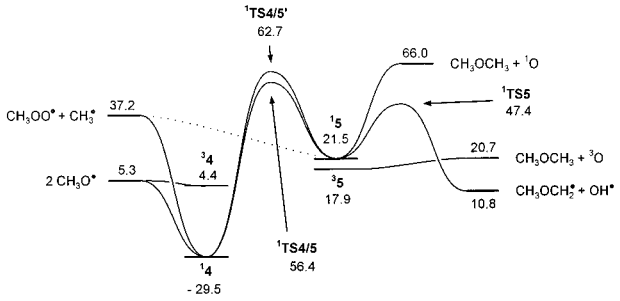

Figure 6. Calculated singlet and triplet potential energy surfaces of the $^1[C_2,H_6,O_2]$ and $^3[C_2,H_6,O_2]$ systems at the BECKE3LYP/6-311++G(d,p) level of theory.

CHART 3

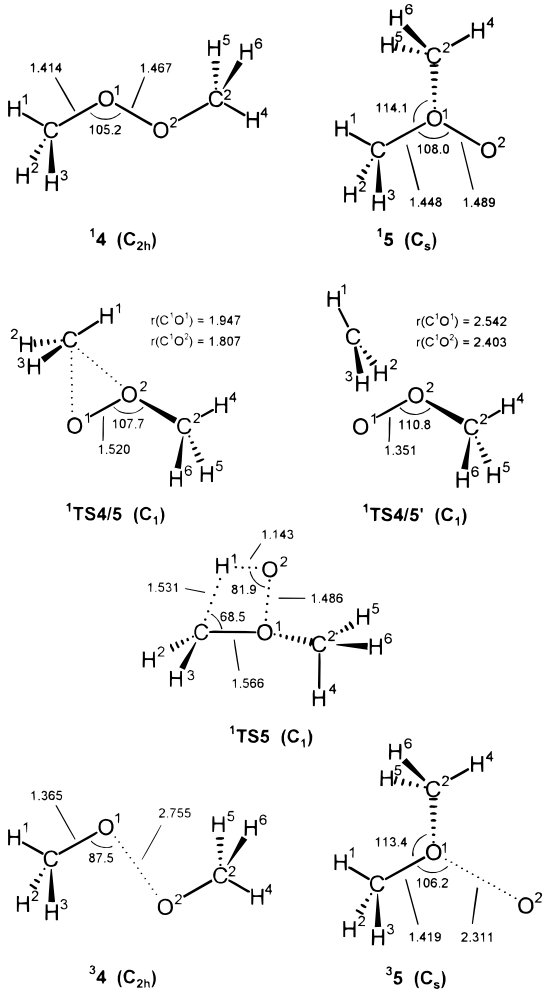

to the flat potential energy surface for rotation about the O−O bond, smaller values for the ∠COOC dihedral have also been reported.[46]

Two transition structures, **^{1}TS4/5** and **^{1}TS4/5′**, describe the 1,2-methyl migrations with either retention or inversion of the configuration at the migrating carbon atom. However, the barrier heights are significant (i.e., 35 kcal/mol for **^{1}TS4/5** and 41 kcal/mol for **^{1}TS4/5′**) relative to dimethyl ether oxide. Thus, methyl substitution does indeed lead to a sizable kinetic stabilization of the ylide, even though the thermochemical stability difference from the conventional peroxide isomer is hardly changed by alkylation. As far as direct bond ruptures are concerned, O−O bond cleavage of **^{1}4** corresponds to the lowest-lying exit channel[47] for which a dissociation energy of 35 kcal/mol is calculated; this value is in agreement with 37 kcal/mol derived from literature data[10] and 39 kcal/mol derived from previous calculations.[38] The loss of a $CH_3^\bullet$ radical concomitant with formation of $CH_3OO^\bullet$ represents the lowest exit channel accessible from dimethyl ether oxide with an energy demand of 16 kcal/mol. Hence, like in the methanol oxide system, the 1,2-migration of the methyl group is much more energy demanding than its loss. The transition structure **^{1}TS5** for decomposition into $CH_3OCH_2^\bullet$ and $OH^\bullet$ radicals is located only 26 kcal/mol above **^{1}5** instead of 35 kcal/mol for methanol oxide.

TABLE 11: Calculated Total Energies (E_t), Zero-point Vibrational Energies (ZPVE), and Calculated and Experimental Heats of Formation (ΔH_f) of Singlet and Triplet $[C_2,H_6,O_2]$ Isomers and Relevant Fragmentation Reactions

isomer/fragment	E_t[a] (Hartree)	ZPVE (Hartree)	ΔH_f[b] (kcal/mol)	ΔH_f[c] (kcal/mol)
^{1}CH_3OOCH_3 ^{1}4	−230.153115	0.081793	−29.5	−30.0
^{1}$(CH_3)_2OO$ ^{1}5	−230.086904	0.083220	21.5	
^{1}TS4/5	−230.030751	0.079640	56.4	
^{1}TS4/5′	−230.020694	0.078126	62.7	
^{1}TS5	−230.030553	0.076628	47.4	
^{3}CH_3OOCH_3 ^{3}4	−230.113696	0.073179	4.4	
^{3}$(CH_3)_2OO$ ^{3}5	−230.092216	0.080292	17.9	
2 $CH_3O^\bullet$	−230.112350	0.072138	5.3	7.4
$CH_3OCH_2^\bullet + OH^\bullet$	−230.103535	0.073791	10.8	
$CH_3OCH_3 + {}^3O$	−230.087762	0.079232	20.7	15.6
$CH_3OO^\bullet + CH_3^\bullet$	−230.061419	0.072353	37.2	37.2
$CH_3OCH_3 + {}^1O$[d]			66.0	60.9
$CH_3OCH_2^+ + OH^-$	−229.906679	0.076962	134.3	

[a] Total energies based on Becke3LYP/6-311++G(d,p)-optimized structures including unscaled ZPVE corrections. [b] Calculated on the basis of literature data for the $CH_3OO^\bullet + CH_3^\bullet$ exit channel. [c] Experimental reference data as given in Table 6 and ref 10. [d] See footnote *d* in Table 7.

As for the other ylides, two weakly bound triplet species, **^{3}4** and **^{3}5**, with dissociation energies of 1 and 3 kcal/mol, respectively, are predicted to exist on the $^3[C_2,H_6,O_2]$ potential energy surface. These species can be described as $^3[CH_3O^\bullet\cdot\cdot OCH_3]$ and $[(CH_3)_2O\cdot{}^3O]$ van der Waals complexes with large O−O distances (2.755 and 2.311 Å). Species **^{3}5** is predicted to be lower in energy than **^{1}5** by 3.6 kcal/mol. Thus, for the question of stability of the singlet molecule, it is important to locate the singlet−triplet crossing point of minimal energy (Table 5). The calculated geometry of the MECP is close to that of singlet dimethyl ether oxide, but with an O−O bond elongated to 1.824 Å. The energy demand at this point amounts to ∼14 kcal/mol relative to **^{1}5**, which is only slightly lower than the methyl loss channel (16 kcal/mol). As the formation of $CH_3^\bullet + CH_3OO^\bullet$ is favored by entropy, it is expected to contribute significantly to the unimolecular chemistry, although the singlet−triplet crossing followed by fragmentation into dimethyl ether and an O (^{3}P) atom may compete to some extent. In conclusion, dimethyl ether oxide is kinetically stabilized by ∼15 kcal/mol against decomposition, rearrangement, and spin crossover. Therefore, it appears as a feasible perspective to generate and isolate ether oxides from appropriate precursors either in gas-phase or rare-gas matrixes.[48]

An experimental characterization by matrix isolation requires a reliable theoretical prediction of the frequencies of **^{1}5** as well as an estimation of the isotopic shifts of these modes. Therefore, frequency calculations were carried out by the BECKE3LYP/6-311++G(d,p) and MP2/6-311++G(d,p) methods (Table 12). Most frequencies and even the IR intensities calculated by both methods are in fair agreement. However, the O−O stretching mode is predicted to be observed at much higher wavenumbers

TABLE 12: Frequencies for (Unlabeled) Dimethyl ether Oxide and Frequency Shifts for ^{2}H- and ^{18}O-Labeled Isotopologues Calculated at the BECKE3LYP/6-311++G(d,p) Level of Theory (MP2/6-311++G(d,p) Frequencies of Unlabeled ^{1}5 Are Given for Comparison)

	$(CH_3)_2OO$ (MP2)		$(CH_3)_2OO$ (B3LYP)		$(CH_3)_2{}^{18}OO$	$(CH_3)_2O{}^{18}O$	$(CH_3)_2{}^{18}O{}^{18}O$	$(CD_3)_2OO$
frequency shift	ν (cm^{-1})[a]	Int. (km/mol)	ν (cm^{-1})[a]	Int. (km/mol)	$\Delta\nu$ (cm^{-1})	$\Delta\nu$ (cm^{-1})	$\Delta\nu$ (cm^{-1})	ν (cm^{-1})[a]
ν_1	3065	(1)	3062	(2)	0	0	0	2275
ν_2	3063	(<1)	3061	(1)	0	0	0	2271
ν_3 CH str	3018	(16)	3012	(25)	0	0	0	2238
ν_4	3016	(7)	3008	(<1)	0	0	0	2235
ν_5 CH str	2917	(33)	2929	(41)	0	0	0	2097
ν_6 CH str	2911	(12)	2920	(16)	0	0	0	2089
ν_7 CH def	1430	(26)	1440	(26)	0	0	0	1081
ν_8	1414	(2)	1424	(3)	−1	0	−1	1062
ν_9 CH def	1406	(10)	1410	(12)	−1	0	−1	1038
ν_{10}	1398	(1)	1404	(3)	0	0	0	1033
ν_{11} CH def	1390	(9)	1393	(11)	0	0	0	1022
ν_{12}	1371	(<1)	1377	(<1)	−2	0	−2	1018
ν_{13}	1197	(1)	1197	(<1)	−8	0	−8	990
ν_{14}	1162	(5)	1157	(5)	−8	0	−8	1005
ν_{15} COC asym str	1153	(38)	1145	(34)	−17	0	−17	938
ν_{16}	1099	(0)	1100	(0)	0	0	0	831
ν_{17} COC asym str	972	(38)	954	(45)	−19	0	−19	787
ν_{18} COC sym str	903	(27)	834	(34)	−18	0	−19	767
ν_{19} OO str	760	(11)	690	(7)	−10	−21	−35	657
ν_{20} COC bend	395	(17)	370	(15)	−2	−1	−6	344
ν_{21} out of plane	410	(8)	370	(2)	−4	−9	−11	316
ν_{22} COO bend	374	(7)	364	(13)	−9	−6	−13	328
ν_{23}	267	(2)	240	(1)	0	−1	−1	177
ν_{24}	217	(<1)	206	(<1)	0	0	0	148

[a] BECKE3LYP frequencies are scaled by a factor of 0.96, MP2 frequencies by a factor of 0.94 (ref 18).

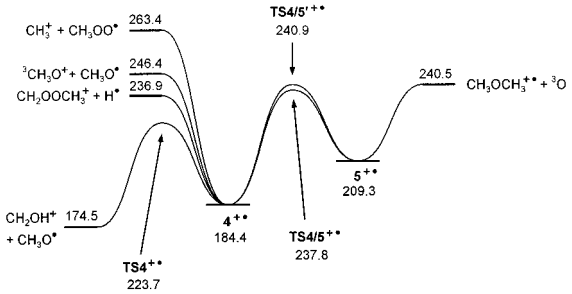

Figure 7. Calculated doublet potential energy surface of the $^2[C_2,H_6,O_2]^{\bullet+}$ system at the BECKE3LYP/6-311++G(d,p) level of theory.

(760 cm^{-1}, ν_{19}) with MP2 compared with the BECKE3LYP result (690 cm^{-1}). Similarly, the COC symmetric stretching (ν_{18}) and the out-of-plane (ν_{21}) vibrations are distinctly different for both methods. As discussed in the previous section dealing with $[H_2,O_2]$, the BECKE3LYP frequencies appear more reliable than those obtained with MP2.

The $^2[C_2,H_6,O_2]^{\bullet+}$ Cation. The $^2[C_2,H_6,O_2]^{\bullet+}$ potential energy surface has been the subject of several theoretical and experimental investigations mostly concerned with ionized ethylene glycol[49] and dimethyl peroxide.[42,50] The parts of this potential energy surface that are relevant for a discussion of ionized dimethyl ether oxide are depicted in Figure 7. With the exception of the 1,2-hydrogen migration, which of course is not possible for ionized dimethyl ether oxide, the situation is again very similar to the ionized methyl hydroperoxide/methanol oxide system. Therefore, only a few aspects will be mentioned here. Isomers **4**$^{\bullet+}$ and **5**$^{\bullet+}$ are connected by two high-energy transition structures (Table 13) for methyl shifts with retention (**TS4/5**$^{\bullet+}$) or inversion (**TS4/5′**$^{\bullet+}$) of configuration at the migrating carbon (Chart 4). The energy gap between the minima of the cation radicals is again much smaller than that of the corresponding neutral species. Considering the high energy demand for methyl migration, the intramolecular isomerization **4**$^{\bullet+}$ → **5**$^{\bullet+}$ will be superseded by two fragmentation pathways that are lower in energy. Thus, loss of a hydrogen atom yielding $CH_3OOCH_2^+$ ions as well as cleavage of the O−O bond with concomitant 1,2-hydrogen migration via **TS4**$^{\bullet+}$ giving rise to CH_2OH^+ and $CH_3O^\bullet$ are expected to contribute to the unimolecular decay of dimethyl peroxide cation radicals. The energy difference between these two channels is larger than that for the analogous $CH_3OOH^{\bullet+} \rightarrow CH_2OOH^+ + H^\bullet$ and $CH_3OOH^{\bullet+} \rightarrow CH_2OH^+ + OH^\bullet$ reactions starting from **1**$^{\bullet+}$. The coupled 1,2-H shift/O−O bond cleavage reaction is the pathway of lower energy for ^{1}**1** as well as ^{1}**4**, whereas loss of atomic hydrogen is entropically favored. Thus, one expects that the O−O bond cleavage competes inefficiently with loss of H$^\bullet$ in the unimolecular decay of **1**$^{\bullet+}$, whereas the amount of O−O bond cleavage relative to the hydrogen abstraction should be larger for **4**$^{\bullet+}$. This result has indeed been described in two

TABLE 13: Calculated Total Energies (E_t), Zero-Point Vibrational Energies (ZPVE), and Calculated as Well as Experimental Heats of Formation (ΔH_f) of Doublet $[C_2,H_6,O_2]^{\bullet+}$ Isomers and Relevant Fragmentation Reactions

isomer/fragment	E_t[a] (Hartree)	ZPVE (Hartree)	ΔH_f[b] (kcal/mol)	ΔH_f[c] (kcal/mol)
$CH_3OOCH_3^{\bullet+}$ 4$^{\bullet+}$	−229.822067	0.081695	184.4	179.8
$(CH_3)_2OO^{\bullet+}$ 5$^{\bullet+}$	−229.782379	0.082206	209.3	
TS4/5$^{\bullet+}$	−229.736937	0.078056	237.8	
TS4/5′$^{\bullet+}$	−229.731960	0.076223	240.9	
TS4$^{\bullet+}$	−229.759370	0.072337	223.7	
$CH_2OCH_3^+ + OH^\bullet$	−229.841728	0.076877	172.0	
$CH_2OH^+ + CH_3O^\bullet$	−229.837784	0.076546	174.5	171.7
$CH_2OOCH_3^+ + H^\bullet$	−229.738354	0.070934	236.9	
$CH_3OCH_3^{\bullet+} + {}^3O$	−229.732678	0.075660	240.5	246.8
$^3CH_3O^+ + CH_3O^\bullet$	−229.723214	0.069205	246.4	251.1
$CH_3^+ + CH_3OO^\bullet$	−229.696172	0.073884	263.4	263.4
$^3CH_3OO^+ + CH_3^\bullet$	−229.684081	0.070941	271.0	274.9
$^1CH_3OO^+ + CH_3^\bullet$	−229.665299	0.071661	282.8	282.3

[a] Total energies based on Becke3LYP/6-311++G(d,p)-optimized structures including unscaled ZPVE corrections. [b] Calculated on the basis of literature data for the $CH_3^+ + CH_3OO^\bullet$ exit channel. [c] Experimental reference data as given in Table 6 and ref 10.

TABLE 14: Reaction Enthalpies for the Rearrangements to the Corresponding Peroxides, Heights of the MECPs, Dissociation Enthalpies for Losses of Triplet Oxygen, and Partial Charges[a] of Singlet and Triplet Water, Methanol, and Dimethyl Ether Oxides[b] and of the Corresponding R_2O Compounds Calculated with BECKE3LYP

	ΔH_R[c]	ΔH_R[c]	E(MECP)[d]	^1R_2OO		^3R_2OO		$^1R_2O + {}^3O$
oxide	$^1R_2OO \rightarrow {}^1ROOR$	$^1R_2OO \rightarrow {}^1R_2O + {}^3O$	$^1R_2OO \rightarrow {}^3R_2OO$	$q_{O(1)}$[e]	$q_{O(2)}$[f]	$q_{O(1)}$[e]	$q_{O(2)}$[f]	$q_{O(1)}$[g]
H_2OO	−45.4	−14.0	6.0	−0.240	−0.562	−0.862	−0.073	−0.916
$CH_3(H)OO$	−55.4	−5.6	10.0	−0.343	−0.553	−0.669	−0.101	−0.732
$(CH_3)_2OO$	−51.0	−0.8	13.6	−0.460	−0.554	−0.534	−0.107	−0.591

[a] According to natural bonding orbital (NBO) population analysis. [b] Calculated dipole moments: $\mu(H_2OO) = 5.1$ D; $\mu(CH_3O(H)O) = 5.2$ D; $\mu((CH_3)_2OO) = 5.1$ D. [c] Reaction enthalpy in kcal/mol at 0 K including unscaled ZPVE. [d] Heights (in kcal/mol) of the minimal energy crossing point (MECP) between the singlet and triplet surface relative to the ^1R_2OO minimum; the 6-31G(d) basis was applied for all except the two oxygen atoms (6-31+G(d)). [e] The index O(1) denotes the oxygen atom bound to the two substituents R (R = H, CH_3). [f] The index O(2) denotes the oxo-oxygen atom. [g] The index O(1) denotes the oxygen atom in the corresponding R_2O compound (R = H, CH_3).

CHART 4

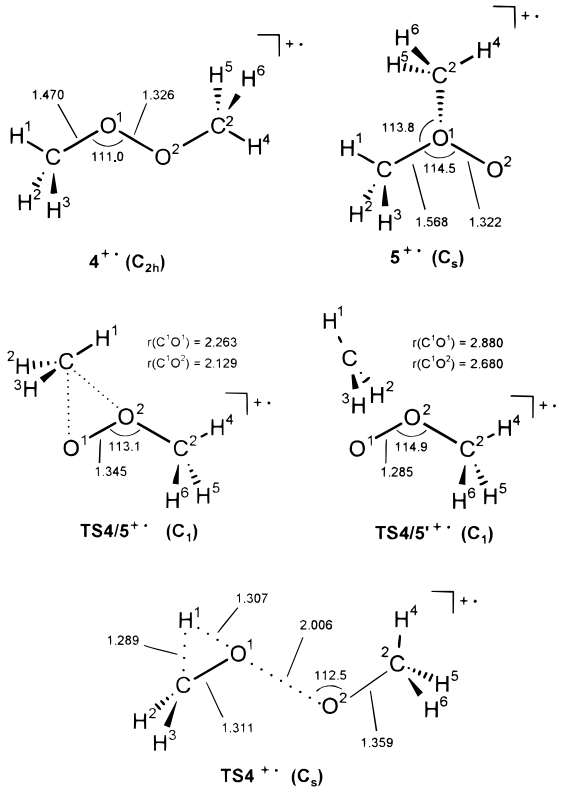

earlier experimental studies dealing with the structure and unimolecular decay of peroxide cation radicals.[42,43]

Concerning the preparation of dimethyl ether oxide, the mass spectrometric approach similar to that used to generate water oxide,[6] involving an isomerization $\mathbf{4}^{\bullet+} \rightarrow \mathbf{5}^{\bullet+}$ is impossible because, as already stated, direct fragmentations of $\mathbf{4}^{\bullet+}$ are more facile than its isomerization. However, the calculations suggest that the neutralization-reionization sequence of the type $^2\mathbf{5}^{\bullet+} \rightarrow {}^1\mathbf{5} \rightarrow {}^2\mathbf{5}^{\bullet+}$ itself is feasible, providing a suitable, pure precursor ion beam of $^2\mathbf{5}^{\bullet+}$ can be generated.

Comparison of the Neutral Ylides. Similar to water oxide, theory predicts neutral methanol and dimethyl ether oxides in their singlet states as stable species resting in local minima ∼45−50 kcal/mol above the corresponding peroxides. Although for water and methanol oxides hydrogen migration is facile and the kinetic stabilization does not exceed ∼5 kcal/mol, intramolecular rearrangement of dimethyl ether oxide is much more energy demanding. In fact, for dimethyl ether oxide, the loss of a methyl radical concomitant with $CH_3OO^{\bullet}$ formation should compete with a crossing to the triplet potential energy surface, leading to the loss of atomic oxygen in its triplet ground state.

As far as the substituent effects going from water oxide to dimethyl ether oxide are concerned (Table 14), the stability differences between the ylide isomers and the conventional peroxides are similar for all three systems considered here. A considerable stabilization of the ylide structures becomes, however, apparent with respect to the losses of triplet oxygen from the ylides (i.e., $^1R_2OO \rightarrow {}^1R_2O + {}^3O$). Although BECKE3LYP predicts an exothermicity of 14.0 kcal/mol for the decomposition of water oxide according to $^1H_2OO \rightarrow {}^1H_2O + {}^3O$, the corresponding exothermicities decrease to 5.6 kcal/mol for methanol oxide and 0.8 kcal/mol for dimethyl ether oxide. Accordingly, the energy demands of the MECPs increase upon alkylation, and the height of the MECP amounts to ∼14 kcal/mol for dimethyl ether oxide. These trends can be attributed to a stabilization of the ylide structures by the electron-donating effects of the methyl substitutents. The ylide character of the $R_2O^+-O^-$ species (R = H, CH_3) is illustrated by the partial charges of the terminal oxygen atoms in the ylides; that is, $H_2O^+-O^-$ (−0.562), $(CH_3)(H)O^+-O^-$ (−0.553), and $(CH_3)_2O^+-O^-$ (−0.554). Thus, the terminal oxo atom is negatively charged in all three species, also leading to similar dipole moments of ∼5.1 (Table 14) for these. However, the partial charges of the central oxygen atoms increase from −0.24 in water oxide to −0.34 and −0.46 in methanol and dimethyl ether oxides, respectively. One would expect a positive charge at the central oxygen atom; however, charge is dispersed to the substituents. The positive character of the central oxygen atom in singlet R_2OO (R = H, CH_3) becomes obvious upon comparison with its loosely bound triplet analogue or the free R_2O units as references. For example, the central oxygen atom in water oxide exhibits a partial charge of −0.24 because of the ylide character, whereas in the loosely bound triplet species, the partial charge increases to −0.862, which is similar to that in free water (−0.916). These trends are comparable for methanol and dimethyl ether oxides (Table 14). Accordingly, electron-withdrawing substituents are expected to destabilize the corresponding ylides, which is unfortunate because otherwise a compound such as $(CF_3)_2OO$ would represent an attractive target for a stable ether oxide with oxidation-resistant substituents.

Conclusions

Methanol and dimethyl ether oxides are predicted to be stable species in the gas phase. The calculations suggest that both species can be probed by NRMS, mass spectrometry, provided that appropriate precursors for the generation of pure beams of the corresponding cation radicals are available. Although these cation radicals are fairly stable toward rearrangement to the corresponding peroxo species, their preparation in a pure form represents a formidable challenge. The simple approach used for the detection of neutral water oxide cannot be applied to

methanol and dimethyl ether oxides because of the unfavorable properties of the anionic potential energy surfaces.

Whereas for water and methanol oxides the 1,2-hydrogen transfer to the corresponding peroxides is facile, complete alkylation in dimethyl ether oxide leads to a significant barrier for intramolecular rearrangement. In fact, the kinetic stability of dimethyl ether oxide against fragmentation, rearrangement to dimethyl peroxide, and with respect to spin crossing leading to the triplet surface is predicted to be sufficient for its generation in rare gas matrixes. The calculated IR spectrum and isotope shifts of the IR frequencies may, hence, allow the identification of matrix isolated dimethyl ether oxide. As precursors, dimethyl ether and ^{1}O atoms produced by photolysis of ozone or dinitrogen oxide might be appropriate. Potential problems of this approach arise from the fact that ^{1}O atoms as well as singlet dimethyl ether oxide are potent oxidation agents and might, therefore, give rise to insertions into C−H bonds. As a result, the competing formation of hydroxymethoxymethane, CH_3OCH_2OH, might suppress the generation of dimethyl ether oxide. However, the consideration of a larger variety of substituents may provide new perspectives and is suggested as a subject for further studies.

To come back to the title question, methanol and dimethyl ether oxides are indeed viable species with considerable ylide character; however, the term "stable" cannot be understood in the common sense of bulk production in laboratory scale. Rather, these species represent highly reactive intermediates. For their characterization sophisticated experiments will be necessary and, in particular, appropriate precursors have still to be found.

Acknowledgment. We are indebted to Prof. W. Sander and Dipl.-Chem. R. Wrobel for intense discussions and many helpful comments on the matrix isolation technique and its potential applicability to the generation of ether oxides. C.A.S. thanks Prof. H. F. Schaefer III for a stimulating discussion on the present topic during the WATOC 1996 conference, Jerusalem. Financial support by the Deutsche Forschungsgemeinschaft, the Fonds der Chemischen Industrie, and the Gesellschaft von Freunden der Technischen Universität Berlin is acknowledged. This paper is dedicated—with admiration—to Professor Rudolf Zahradnik, Praha, on the occasion of his 70th birthday.

Appendix

For clarity, we reduced the calculated geometrical data presented in the Charts to the most important features. Here, the complete set of data is given (bond distances in Å, bond angles in degrees) as derived at the BECKE3LYP/6-311++G(d,p) level of theory. Numbers of atoms are used as shown in the Charts.

^{1}CH$_3$OOH, ^{1}1: C_1 symmetry; r(OO) = 1.460; r(CO^1) = 1.417; r(O^{2}H^4) = 0.967; r(CH^1) = 1.092; r(CH^2) = 1.094; r(CH^3) = 1.095; ∠COO = 106.0; ∠O^{1}O^{2}H^4 = 100.0; ∠H^{1}CO^1 = 104.3; ∠H^{2}CO^1 = 111.0; ∠H^{3}CO^1 = 111.4; ∠H^{1}CH^2 = 109.7; ∠H^{1}CH^3 = 110.1; ∠H^{2}CH^3 = 110.1; ∠CO^{1}O^{2}H^4 = −134.6; ∠H^{1}CO^{1}O^2 = −177.5; ∠H^{2}CO^{1}O^2 = −59.4; ∠H^{3}CO^{1}O^2 = 63.7.

^{1}CH$_3$(H)OO, ^{1}2: C_1 symmetry; r(OO) = 1.511; r(CO^1) = 1.453; r(O^{1}H^4) = 0.969; r(CH^1) = 1.092; r(CH^2) = 1.085; r(CH^3) = 1.089; ∠COO = 109.4; ∠O^{2}O^{1}H^4 = 102.8; ∠CO^{1}H^4 = 110.0; ∠H^{1}CO^1 = 107.7; ∠H^{2}CO^1 = 105.0; ∠H^{3}CO^1 = 109.0; ∠H^{1}CH^2 = 111.5; ∠H^{1}CH^3 = 112.8; ∠H^{2}CH^3 = 110.6; ∠H^{1}CO^{1}O^2 = 176.2; ∠H^{1}CO^{1}H^4 = 64.0; ∠H^{2}CO^{1}O^2 = −64.9; ∠H^{3}CO^{1}O^2 = 53.6.

^{1}TS1/2-H: C_1 symmetry; r(OO) = 1.598; r(CO^1) = 1.440; r(O^{1}H^4) = 1.046; r(O^{2}H^4) = 1.355; r(CH^1) = 1.092; r(CH^2) = 1.089; r(CH^3) = 1.090; ∠COO = 107.6; ∠O^{1}O^{2}H^4 = 40.5; ∠O^{2}H^{4}O^1 = 82.4; ∠H^{4}O^{1}O^2 = 57.2; ∠CO^{1}H^4 = 114.4; ∠H^{1}CO^1 = 106.2; ∠H^{2}CO^1 = 107.1; ∠H^{3}CO^1 = 110.4; ∠H^{1}CH^2 = 111.0; ∠H^{1}CH^3 = 110.3; ∠H^{2}CH^3 = 110.4; ∠H^{1}CO^{1}O^2 = 173.6; ∠H^{1}CO^{1}H^4 = 112.3; ∠H^{2}CO^{1}O^2 = −67.7; ∠H^{3}CO^{1}O^2 = 52.5.

^{1}TS1/2-CH$_3$: C_1 symmetry; r(OO) = 1.541; r(CO^1) = 1.946; r(CO^2) = 1.819; r(O^{2}H^4) = 0.970; r(CH^1) = 1.091; r(CH^2) = 1.079; r(CH^3) = 1.082; ∠CO^{1}O^2 = 61.6; ∠O^{1}CO^2 = 48.2; ∠CO^{2}O^1 = 70.2; ∠O^{1}O^{2}H^4 = 101.5; ∠CO^{2}H^4 = 111.0; ∠H^{1}CO^1 = 136.7; ∠H^{2}CO^1 = 89.9; ∠H^{3}CO^1 = 86.2; ∠H^{1}CO^2 = 89.5; ∠H^{2}CO^2 = 89.9; ∠H^{3}CO^2 = 118.9; ∠H^{1}CH^2 = 113.1; ∠H^{1}CH^3 = 113.2; ∠H^{2}CH^3 = 114.9; ∠CO^{1}O^{2}H^4 = −180.4; ∠H^{1}CO^{1}O^2 = 14.8; ∠H^{2}CO^{1}O^2 = −109.9; ∠H^{3}CO^{1}O^2 = 135.2.

^{1}TS1/2-CH$_3$′: C_1 symmetry; r(OO) = 1.361; r(CO^1) = 2.538; r(CO^2) = 2.396; r(O^{2}H^4) = 0.975; r(CH^1) = 1.087; r(CH^2) = 1.072; r(CH^3) = 1.073; ∠CO^{1}O^2 = 68.3; ∠O^{1}CO^2 = 31.9; ∠CO^{2}O^1 = 79.8; ∠O^{1}O^{2}H^4 = 106.1; ∠CO^{2}H^4 = 102.0; ∠H^{1}CO^1 = 170.9; ∠H^{2}CO^1 = 61.2; ∠H^{3}CO^1 = 59.9; ∠H^{1}CO^2 = 157.2; ∠H^{2}CO^2 = 63.4; ∠H^{3}CO^2 = 67.9; ∠H^{1}CH^2 = 119.3; ∠H^{1}CH^3 = 118.7; ∠H^{2}CH^3 = 121.0; ∠CO^{1}O^{2}H^4 = 99.7; ∠H^{1}CO^{1}O^2 = −179.4; ∠H^{2}CO^{1}O^2 = 85.3; ∠H^{3}CO^{1}O^2 = −96.2.

^{1}TS2: C_1 symmetry; r(OO) = 1.495; r(CO^1) = 1.566; r(O^{1}H^4) = 0.971; r(O^{2}H^1) = 1.150; r(CH^1) = 1.533; r(CH^2) = 1.094; r(CH^3) = 1.090; ∠COO = 95.3; ∠O^{1}O^{2}H^4 = 111.1; ∠H^{1}CO^1 = 68.7; ∠O^{2}H^{1}C = 114.4; ∠O^{1}O^{2}H^1 = 81.6; ∠H^{2}CO^1 = 105.3; ∠H^{3}CO^1 = 102.3; ∠H^{1}CH^2 = 124.6; ∠H^{1}CH^3 = 124.4; ∠H^{2}CH^3 = 110.8; ∠H^{1}CO^{1}O^2 = 1.1; ∠H^{1}O^{2}O^{1}H^4 = 114.1; ∠H^{2}CO^{1}O^2 = 120.9; ∠H^{3}CO^{1}O^2 = −123.0.

^{3}CH$_3$OOH, ^{3}1: C_1 symmetry; r(OO) = 2.175; r(CO^1) = 1.372; r(O^{2}H^4) = 0.971; r(CH^1) = 1.097; r(CH^2) = 1.097; r(CH^3) = 1.107; ∠COO = 100.8; ∠O^{1}O^{2}H^4 = 86.4; ∠H^{1}CO^1 = 112.1; ∠H^{2}CO^1 = 111.4; ∠H^{3}CO^1 = 105.8; ∠H^{1}CH^2 = 112.9; ∠H^{1}CH^3 = 108.2; ∠H^{2}CH^3 = 105.9; ∠CO^{1}O^{2}H^4 = −176.6; ∠H^{1}CO^{1}O^2 = −160.6; ∠H^{2}CO^{1}O^2 = −32.9; ∠H^{3}CO^{1}O^2 = 81.7.

^{3}CH$_3$(H)OO, ^{3}2: C_1 symmetry; r(OO) = 2.339; r(CO^1) = 1.428; r(O^{1}H^4) = 0.963; r(CH^1) = 1.096; r(CH^2) = 1.095; r(CH^3) = 1.089; ?COO = 108.0; ?O^{2}O^{1}H^4 = 84.9; ?CO^{1}H^4 = 109.6; ?H^{1}CO^1 = 111.1; ?H^{2}CO^1 = 111.9; ?H^{3}CO^1 = 106.5; ?H^{1}CH^2 = 109.3; ?H^{1}CH^3 = 109.0; ?H^{2}CH^3 = 108.9; ?H^{1}CO^{1}O^2 = −156.5; ?H^{1}CO^{1}H^4 = −65.6; ?H^{2}CO^{1}O^2 = −34.0; ?H^{3}CO^{1}O^2 = 84.9.

MECP (smaller basis set, see text): C_1 symmetry; r(OO) = 1.795; r(CO^1) = 1.440; r(O^{1}H^4) = 0.972; r(CH^1) = 1.095; r(CH^2) = 1.089; r(CH^3) = 1.092; ∠COO = 106.7; ∠O^{2}O^{1}H^4 = 96.6; ∠CO^{1}H^4 = 111.3; ∠H^{1}CO^1 = 108.7; ∠H^{2}CO^1 = 105.3; ∠H^{3}CO^1 = 110.6; ∠H^{1}CH^2 = 110.7; ∠H^{1}CH^3 = 111.3; ∠H^{2}CH^3 = 110.0; ∠H^{1}CO^{1}O^2 = 176.1; ∠H^{1}CO^{1}H^4 = 71.9; ∠H^{2}CO^{1}O^2 = −65.2; ∠H^{3}CO^{1}O^2 = 53.6.

CH$_3$OOH$^{\bullet+}$, 1$^{\bullet+}$: C_1 symmetry; r(OO) = 1.324; r(CO^1) = 1.465; r(O^{2}H^4) = 0.990; r(CH^1) = 1.092; r(CH^2) = 1.088; r(CH^3) = 1.097; ∠COO = 111.6; ∠O^{1}O^{2}H^4 = 104.1; ∠H^{1}CO^1 = 103.5; ∠H^{2}CO^1 = 109.2; ∠H^{3}CO^1 = 105.0; ∠H^{1}CH^2 = 110.7; ∠H^{1}CH^3 = 114.5; ∠H^{2}CH^3 = 112.9; ∠CO^{1}O^{2}H^4 = −178.7; ∠H^{1}CO^{1}O^2 = −143.9; ∠H^{2}CO^{1}O^2 = −21.3; ∠H^{3}CO^{1}O^2 = 100.0.

CH$_3$(H)OO$^{\bullet+}$, 2$^{\bullet+}$: C_1 symmetry; r(OO) = 1.333; r(CO^1) = 1.544; r(O^{1}H^4) = 0.988; r(CH^1) = 1.088; r(CH^2) = 1.086; r(CH^3) = 1.087; ∠COO = 120.7; ∠O^{2}O^{1}H^4 = 113.2; ∠CO^{1}H^4

= 122.7; ∠H¹CO¹ = 103.2; ∠H²CO¹ = 103.1; ∠H³CO¹ = 105.6; ∠H¹CH² = 113.7; ∠H¹CH³ = 114.8; ∠H²CH³ = 114.6; ∠H¹CO¹O² = −161.1; ∠H¹CO¹H⁴ = 41.2; ∠H²CO¹O² = −42.5; ∠H³CO¹O² = 78.9.

TS1/2-H$^{\bullet+}$: C_1 symmetry; r(OO) = 1.391; r(CO¹) = 1.517; r(O¹H⁴) = 1.156; r(O²H⁴) = 1.277; r(CH¹) = 1.089; r(CH²) = 1.089; r(CH³) = 1.089; ∠COO = 116.9; ∠O¹O²H⁴ = 51.1; ∠O²H⁴O¹ = 69.6; ∠H⁴O¹O² = 59.3; ∠CO¹H⁴ = 145.2; ∠H¹CO¹ = 102.3; ∠H²CO¹ = 104.5; ∠H³CO¹ = 106.4; ∠H¹CH² = 114.2; ∠H¹CH³ = 113.9; ∠H²CH³ = 114.9; ∠H¹CO¹O² = −163.2; ∠H¹CO¹H⁴ = 122.7; ∠H²CO¹O² = −43.9; ∠H³CO¹O² = 77.1.

TS1/2-CH$_3^{\bullet+}$: C_1 symmetry; r(OO) = 1.346; r(CO¹) = 2.396; r(CO²) = 2.220; r(O²H⁴) = 0.985; r(CH¹) = 1.086; r(CH²) = 1.087; r(CH³) = 1.087; ∠CO¹O² = 66.0; ∠O¹CO² = 33.6; ∠CO²O¹ = 80.4; ∠O¹O²H⁴ = 108.3; ∠CO²H⁴ = 149.9; ∠H¹CO¹ = 117.2; ∠H²CO¹ = 84.0; ∠H³CO¹ = 78.3; ∠H¹CO² = 85.2; ∠H²CO² = 91.3; ∠H³CO² = 103.1; ∠H¹CH² = 119.8; ∠H¹CH³ = 119.9; ∠H²CH³ = 119.4; ∠CO¹O²H⁴ = −150.2; ∠H¹CO¹O² = 19.0; ∠H²CO¹O² = −101.5; ∠H³CO¹O² = 136.8.

TS1/2-CH$_3'^{\bullet+}$: C_s symmetry; r(OO) = 1.306; r(CO¹) = 2.926; r(CO²) = 2.687; r(O²H⁴) = 0.986; r(CH¹) = 1.090; r(CH²) = 1.085; ∠CO¹O² = 66.5; ∠O¹CO² = 26.5; ∠CO²O¹ = 87.0; ∠O¹O²H⁴ = 108.7; ∠CO²H⁴ = 164.3; ∠H¹CO¹ = 178.8; ∠H²CO¹ = 60.5; ∠H¹CO² = 154.7; ∠H²CO² = 63.8; ∠H¹CH² = 119.7; ∠H²CH³ = 120.5; ∠CO¹O²H⁴ = 180.0; ∠H¹CO¹O² = 180.0; ∠H²CO¹O² = 90.0.

TS1$^{\bullet+}$: C_s symmetry; r(OO) = 1.950; r(CO¹) = 1.311; r(O¹H¹) = 1.395; r(O²H⁴) = 0.988; r(CH¹) = 1.257; r(CH²) = 1.095; ∠CO¹O² = 112.9; ∠CO¹H¹ = 55.2; ∠O¹H¹C = 59.0; ∠H¹CO¹ = 65.8; ∠O¹O²H⁴ = 102.1; ∠H¹O¹O² = 168.1; ∠H²CO¹ = 118.7; ∠H¹CH² = 108.1; ∠H²CH³ = 120.6; ∠CO¹O²H⁴ = 180.0; ∠H¹CO¹O² = 180.0; ∠H²CO¹O² = 81.8.

CH$_3$O$^{\bullet-}$ HO$^{\bullet}$, 3$^{\bullet-}$: C_1 symmetry; r(CO¹) = 1.366; r(O¹H⁴) = 1.424; r(O²H⁴) = 1.066; r(CH¹) = 1.117; r(CH²) = 1.120; r(CH³) = 1.120; ∠CO¹H⁴ = 115.2; ∠O¹H⁴O² = 179.5; ∠H¹CO¹ = 113.9; ∠H²CO¹ = 113.7; ∠H³CO¹ = 113.6; ∠H¹CH² = 105.1; ∠H¹CH³ = 105.2; ∠H²CH³ = 104.5; ∠CO¹H⁴O² = 33.7; ∠H¹CO¹H⁴ = 4.6; ∠H²CO¹H⁴ = −115.8; ∠H³CO¹H⁴ = 124.9.

^{1}CH$_3$OOCH$_3$, ^{1}4: C_{2h} symmetry; r(OO) = 1.467; r(C¹O¹) = 1.414; r(C¹H¹) = 1.095; r(C¹H²) = 1.092; ∠C¹O¹O² = 105.2; ∠H¹C¹O¹ = 111.2; ∠H²C¹O¹ = 104.6; ∠H¹C¹H² = 109.6; ∠H²C¹H³ = 109.6; ∠COOC = 180.0; ∠H¹C¹O¹O² = 61.5; ∠H²C¹O¹O² = 180.0

^{1}(CH$_3$)$_2$OO, ^{1}5: C_s symmetry; r(OO) = 1.489; r(C¹O¹) = 1.448; r(C¹H¹) = 1.092; r(C¹H²) = 1.091; r(C¹H³) = 1.085; ∠C¹O¹O² = 108.0; ∠C¹O¹C² = 114.1; ∠H¹C¹O¹ = 107.8; ∠H²C¹O¹ = 108.7; ∠H³C¹O¹ = 105.2; ∠H¹C¹H² = 112.5; ∠H¹C¹H³ = 111.7; ∠H²C¹H³ = 110.7; ∠H¹C¹O¹O² = 178.8; ∠H¹C¹O¹C² = −61.1; ∠H²C¹O¹O² = −59.4; ∠H³C¹O¹O² = 59.5.

^{1}TS4/5: C_1 symmetry; r(OO) = 1.520; r(C¹O¹) = 1.947; r(C¹O²) = 1.807; r(C²O²) = 1.422; r(C¹H¹) = 1.091; r(C¹H²) = 1.080; r(C¹H³) = 1.082; r(C²H⁴) = 1.093; r(C²H⁵) = 1.093; r(C²H⁶) = 1.093; ∠C¹O¹O² = 61.4; ∠O¹C¹O² = 47.6; ∠C¹O²O¹ = 71.0; ∠O¹O²C² = 107.7; ∠C¹O²C² = 120.6; ∠H¹C¹O¹ = 135.0; ∠H²C¹O¹ = 93.1; ∠H³C¹O¹ = 85.2; ∠H¹CO² = 90.0; ∠H²C¹O² = 121.4; ∠H³CO² = 102.3; ∠H¹C¹H² = 113.3; ∠H¹C¹H³ = 112.8; ∠H²C¹H³ = 114.6; ∠H⁴C²O² = 106.9; ∠H⁵C²O² = 107.4; ∠H⁶C²O² = 111.2; ∠H⁴C²H⁵ = 110.3; ∠H⁴C²H⁶ = 111.0; ∠H⁵C²H⁶ = 109.5; ∠COOC = −117.1; ∠H¹C¹O¹O² = 24.0; ∠H²C¹O¹O² = −103.8; ∠H³C¹O¹O² = 141.7; ∠H⁴C²O²O¹ = −179.1; ∠H⁵C²O²O¹ = −60.2; ∠H⁶C²O²O¹ = 59.6.

^{1}TS4/5′: C_1 symmetry; r(OO) = 1.351; r(C¹O¹) = 2.542; r(C¹O²) = 2.403; r(C²O²) = 1.442; r(C¹H¹) = 1.087; r(C¹H²) = 1.072; r(C¹H³) = 1.072; r(C²H⁴) = 1.090; r(C²H⁵) = 1.092; r(C²H⁶) = 1.092; ∠C¹O¹O² = 68.5; ∠O¹C¹O² = 31.5; ∠C¹O²O¹ = 79.9; ∠O¹O²C² = 110.8; ∠C¹O²C² = 112.6; ∠H¹C¹O¹ = 170.1; ∠H²C¹O¹ = 62.0; ∠H³C¹O¹ = 59.1; ∠H¹CO² = 158.3; ∠H²C¹O² = 63.7; ∠H³CO² = 66.9; ∠H¹CH² = 118.5; ∠H¹CH³ = 119.5; ∠H²CH³ = 121.0; ∠H⁴C²O² = 106.1; ∠H⁵C²O² = 108.2; ∠H⁶C²O² = 110.1; ∠H⁴C²H⁵ = 111.0; ∠H⁴C²H⁶ = 111.6; ∠H⁵C²H⁶ = 109.6; ∠COOC = 110.5; ∠H¹C¹O¹O² = 173.5; ∠H²C¹O¹O² = −91.0; ∠H³C¹O¹O² = 89.3; ∠H⁴C²O²O¹ = −171.2; ∠H⁵C²O²O¹ = 69.5; ∠H⁶C²O²O¹ = −50.4.

^{1}TS5: C_1 symmetry; r(OO) = 1.486; r(C¹O¹) = 1.566; r(O¹C²) = 1.450; r(O²H¹) = 1.143; r(C¹H¹) = 1.531; r(C¹H²) = 1.094; r(C¹H³) = 1.092; r(C²H⁴) = 1.089; r(C²H⁵) = 1.090; r(C²H⁶) = 1.087; ∠C¹O¹O² = 95.3; ∠O¹O²C² = 116.8; ∠H¹C¹O¹ = 68.5; ∠O²H¹C¹ = 114.3; ∠O¹O²H¹ = 81.9; ∠H²C¹O¹ = 105.2; ∠H³C¹O¹ = 102.8; ∠H¹C¹H² = 126.8; ∠H¹C¹H³ = 122.7; ∠H²C¹H³ = 110.4; ∠H⁴C²O¹ = 105.7; ∠H⁵C²O¹ = 109.2; ∠H⁶C²O¹ = 106.9; ∠H⁴C²H⁵ = 112.1; ∠H⁴C²H⁶ = 111.4; ∠H⁵C²H⁶ = 111.3; ∠H¹C¹O¹O² = 0.4; ∠H¹C¹O¹C² = −113.0; ∠H²C¹O¹C² = −120.1; ∠H³C¹O¹C² = −124.4; ∠H⁴C²O¹O² = 179.1; ∠H⁴C²O¹C¹ = −75.0; ∠H⁵C²O¹O² = −60.1; ∠H⁶C²O¹O² = 60.4.

^{3}CH$_3$OOCH$_3$, ^{3}4: C_{2h} symmetry; r(OO) = 2.755; r(C¹O¹) = 1.365; r(C¹H¹) = 1.098; r(C¹H²) = 1.102; ∠C¹O¹O² = 87.5; ∠H¹C¹O¹ = 114.2; ∠H²C¹O¹ = 107.1; ∠H¹C¹H² = 111.8; ∠H²C¹H³ = 103.3; ∠COOC = 180.0; ∠H¹C¹O¹O² = 180.0; ∠H²C¹O¹O² = 64.3

^{3}(CH$_3$)$_2$OO, ^{3}5: C_s symmetry; r(OO) = 2.311; r(C¹O¹) = 1.419; r(C¹H¹) = 1.098; r(C¹H²) = 1.097; r(C¹H³) = 1.089; ∠C¹O¹O² = 106.2; ∠C¹O¹C² = 113.4; ∠H¹C¹O¹ = 110.5; ∠H²C¹O¹ = 111.3; ∠H³C¹O¹ = 107.0; ∠H¹C¹H² = 109.1; ∠H¹C¹H³ = 109.6; ∠H²C¹H³ = 109.3; ∠H¹C¹O¹O² = 179.1; ∠H¹C¹O¹C² = −62.8; ∠H²C¹O¹O² = −57.8; ∠H³C¹O¹O² = −61.6.

MECP (smaller basis set, see text): C_s symmetry; r(OO) = 1.824; r(C¹O¹) = 1.433; r(C¹H¹) = 1.096; r(C¹H²) = 1.095; r(C¹H³) = 1.089; ∠C¹O¹O² = 104.8; ∠C¹O¹C² = 114.6; ∠H¹C¹O¹ = 108.7; ∠H²C¹O¹ = 110.2; ∠H³C¹O¹ = 106.0; ∠H¹C¹H² = 110.9; ∠H¹C¹H³ = 110.6; ∠H²C¹H³ = 110.3; ∠H¹C¹O¹O² = 179.1; ∠H¹C¹O¹C² = −66.6; ∠H²C¹O¹O² = −59.1; ∠H³C¹O¹O² = 60.2.

CH$_3$OOCH$_3^{\bullet+}$, 4$^{\bullet+}$: C_{2h} symmetry; r(OO) = 1.326; r(CO) = 1.470; r(CH¹) = 1.091; r(CH³) = 1.088; ∠COO = 111.0; ∠H¹CO = 107.9; ∠H³CO = 102.8; ∠H¹CH² = 112.2; ∠H¹CH³ = 112.7; ∠COOC = 180.0; ∠H¹COO = 60.7; ∠H³COO = 180.0

(CH$_3$)$_2$OO$^{\bullet+}$, 5$^{\bullet+}$: C_s symmetry; r(OO) = 1.322; r(C¹O¹) = 1.568; r(C¹H¹) = 1.115; r(C¹H²) = 1.112; r(C¹H³) = 1.116; ∠C¹O¹O² = 114.5; ∠C¹O¹C² = 113.8; ∠H¹C¹O¹ = 100.3; ∠H²C¹O¹ = 105.3; ∠H³C¹O¹ = 103.6; ∠H¹C¹H² = 115.6; ∠H¹C¹H³ = 114.8; ∠H²C¹H³ = 114.5; ∠H¹C¹O¹O² = 159.3; ∠H¹C¹O¹C² = −66.3; ∠H²C¹O¹O² = −80.1; ∠H³C¹O¹O² = 40.5.

TS4/5$^{\bullet+}$: C_1 symmetry; r(OO) = 1.345; r(C¹O¹) = 2.263; r(C¹O²) = 2.129; r(C²O²) = 1.474; r(C¹H¹) = 1.084; r(C¹H²) = 1.085; r(C¹H³) = 1.085; r(C²H⁴) = 1.088; r(C²H⁵) = 1.091; r(C²H⁶) = 1.089; ∠C¹O¹O² = 66.8; ∠O¹C¹O² = 35.5; ∠C¹O²O¹ = 77.7; ∠O¹O²C² = 113.1; ∠C¹O²C² = 145.5; ∠H¹C¹O¹ = 118.5; ∠H²C¹O¹ = 87.1; ∠H³C¹O¹ = 79.1; ∠H¹CO² = 58.5; ∠H²C¹O² = 106.7; ∠H³CO² = 92.7; ∠H¹C¹H² = 119.4;

$\angle H^1C^1H^3 = 119.2$; $\angle H^2C^1H^3 = 119.1$; $\angle H^4C^2O^2 = 104.7$; $\angle H^5C^2O^2 = 106.0$; $\angle H^6C^2O^2 = 108.7$; $\angle H^4C^2H^5 = 112.2$; $\angle H^4C^2H^6 = 112.8$; $\angle H^5C^2H^6 = 111.9$; $\angle COOC = -145.5$; $\angle H^1C^1O^1O^2 = 23.4$; $\angle H^2C^1O^1O^2 = -98.8$; $\angle H^3C^1O^1O^2 = 140.8$; $\angle H^4C^2O^2O^1 = -169.8$; $\angle H^5C^2O^2O^1 = -51.1$; $\angle H^6C^2O^2O^1 = 69.4$.

TS4/5′$^{\bullet+}$: C_s symmetry; r(OO) = 1.285; r(C^1O^1) = 2.880; r(C^1O^2) = 2.680; r(C^2O^2) = 1.498; r(C^1H^1) = 1.088; r(C^1H^2) = 1.082; r(C^2H^4) = 1.086; r(C^2H^5) = 1.088; $\angle C^1O^1O^2 = 68.0$; $\angle O^1C^1O^2 = 26.4$; $\angle C^1O^2O^1 = 85.6$; $\angle O^1O^2C^2 = 114.9$; $\angle C^1O^2C^2 = 159.6$; $\angle H^1C^1O^1 = 178.2$; $\angle H^2C^1O^1 = 60.7$; $\angle H^3C^1O^1 = 60.0$; $\angle H^1CO^2 = 155.4$; $\angle H^2C^1O^2 = 63.9$; $\angle H^3CO^2 = 63.6$; $\angle H^1CH^2 = 119.6$; $\angle H^2CH^3 = 120.7$; $\angle H^4C^2O^2 = 103.6$; $\angle H^5C^2O^2 = 107.0$; $\angle H^4C^2H^5 = 112.9$; $\angle H^5C^2H^6 = 112.8$; $\angle COOC = 180.0$; $\angle H^1C^1O^1O^2 = 180.0$; $\angle H^2C^1O^1O^2 = -90.6$; $\angle H^4C^2O^2O^1 = 180.$; $\angle H^5C^2O^2O^1 = 59.2$.

TS4$^{\bullet+}$: C_s symmetry; r(C^1O^1) = 1.311; r(C^2O^2) = 1.359; r(O^1O^2) = 2.006; r(C^1H^1) = 1.094; r(C^1H^3) = 1.289; r(H^3O^1) = 1.307; r(C^2H^4) = 1.094; r(C^2H^5) = 1.110; $\angle H^1C^1O^1 = 119.0$; $\angle H^1C^1H^2 = 120.6$; $\angle H^3C^1O^1 = 60.3$; $\angle H^1C^1H^3 = 109.3$; $\angle C^1H^3O^1 = 60.7$; $\angle H^3O^1C^1 = 59.0$; $\angle C^1O^1O^2 = 112.1$; $\angle O^1O^2C^2 = 112.5$; $\angle H^4C^2O^2 = 114.2$; $\angle H^5C^2O^2 = 107.4$; $\angle H^4C^2H^5 = 111.8$; $\angle H^5C^2H^6 = 103.4$; $\angle H^1C^1O^1O^2 = 113.0$; $\angle H^3C^1O^1O^2 = 180.0$; $\angle C^1O^1O^2C^2 = 180.0$; $\angle O^1O^2C^2H^4 = 0.0$; $\angle O^1O^2C^2H^5 = -125.0$.

References and Notes

(1) For selected examples, see: (a) Musher, J. I. *Angew. Chem.* **1969**, *81*, 68; *Angew. Chem., Int. Ed. Engl.* **1969**, *8*, 54; (b) Stang, P. J.; Tykwinski, R. R.; Zhdankin, V. V. *J. Org. Chem.* **1992**, *52*, 1861; (c) Kost, D.; Kalikhman, I.; Raban, M. *J. Am. Chem. Soc.* **1995**, *117*, 11512; (d) Wang, S. L.; Ledingham, K. W. D.; Singhal, R. P. *J. Phys. Chem.* **1996**, *100*, 11282; (e) Hashimoto, M.; Yokoyama, K.; Kudo, H.; Wu, C. H.; Schleyer, P. v. R. *J. Phys. Chem.* **1996**, *100*, 15770; (f) Varvoglis, A. *Hypervalent Iodine in Organic Synthesis*, Academic: New York, 1997.

(2) (a) Bach, R. D.; Owensby, A. L.; Gonzalez, C.; Schlegel, H. B. *J. Am. Chem. Soc.* **1991**, *113*, 6001; (b) Bach, R. D.; Owensby, A. L.; Andres, J. L.; Schlegel, H. B. *J. Am. Chem. Soc.* **1991**, *113*, 7031; (c) Bach, R. D.; Andres, J. L.; Owensby, A. L.; Schlegel, H. B.; McDuall, J. J. W. *J. Am. Chem. Soc.* **1992**, *114*, 7207; (d) Bach, R. D.; Su, M.-D.; Schlegel, H. B. *J. Am. Chem. Soc.* **1994**, *116*, 5379; (e) Bach, R. D.; Su, M.-D. *J. Am. Chem. Soc.* **1994**, *116*, 5392.

(3) Newcomb, M.; Le Tadic-Biadatti, M.-H.; Chestney, D. L.; Roberts, E. S.; Hollenberg, P. F. *J. Am. Chem. Soc.* **1995**, *117*, 12085.

(4) (a) Bach, R. D.; Su, M.-D.; Andres, J. L.; Schlegel, H. B. *J. Am. Chem. Soc.* **1993**, *115*, 8763; (b) Schalley, C. A.; Wesendrup, R.; Schröder, D.; Schwarz, H. *Organometallics* **1996**, *15*, 678; (c) Schalley, C. A. *Gas-Phase Ion Chemistry of Peroxides*, Ph.D. Thesis, TU Berlin D83, Shaker: Herzogenrath/Germany, 1997.

(5) See, for example: (a) Cremer, D. In *The Chemistry of Peroxides*; Patai, S., Ed.; Wiley: New York, 1983; p 1; (b) Pople, J. A.; Raghavachari, K.; Frisch, M. J.; Binkley, J. S.; Schleyer, P. v. R. *J. Am. Chem. Soc.* **1983**, *105*, 6389; (c) Meredith, C.; Hamilton, T. P.; Schaefer, H. F., III *J. Chem. Phys.* **1992**, *96*, 9250; (d) Huang, H. H.; Xie, Y.; Schaefer, H. F., III *J. Phys. Chem.* **1996**, *100*, 6076; (e) Vincent, M. A.; Burton, N. A.; Hillier, I. H. *Mol. Phys.* **1996**, *87*, 945.

(6) Schröder, D.; Schalley, C. A.; Hrušák, J.; Goldberg, N.; Schwarz, H. *Chem. Eur. J.* **1996**, *2*, 1235.

(7) For recent reviews on NR mass spectrometry see: (a) McLafferty, F. W., *Science* **1990**, *247*, 925; (b) McLafferty, F. W. *Int. J. Mass Spectrom. Ion Processes* **1992**, *118/119*, 221; (c) Turecek, F. *Org. Mass Spectrom.* **1992**, *27*, 1087; (d) Goldberg, N.; Schwarz, H. *Acc. Chem. Res* **1994**, *27*, 347; (e) Zagorevskii, D. V.; Holmes, J. L. *Mass Spectrom. Rev.* **1994**, *13*, 133; (f) Polce, M. J.; Beranová, S.; Nold, M. J.; Wesdemiotis, C. *J. Mass Spectrom.* **1996**, *31*, 1073.

(8) (a) Cremer, D. *J. Chem. Phys.* **1978**, *69*, 4440; (b) Frisch, M. J.; Raghavachari, K.; Pople, J. A.; Bouma, W. J.; Radom, L. *Chem. Phys.* **1983**, *75*, 323; (c) Xie, Y.; Allen, W. D.; Yamaguchi, Y.; Schaefer III, H. F. *J. Chem. Phys*, **1996**, *104*, 7615.

(9) (a) Benassi, R.; Taddei, F. *Chem. Phys. Lett.* **1993**, *204*, 595; (b) Humbel, S.; Demachy, I.; Hiberty, P. C. *Chem. Phys. Lett.* **1995**, *247*, 126; (c) Hrušák, J.; Friedrichs, H.; Schwarz, H.; Razafinjanahary, H.; Chermette, H. *J. Phys. Chem.* **1996**, *100*, 100; For experimental studies see: (d) van Doren, J. M.; Barlow, S. E.; DePuy, C. H.; Bierbaum, V. M. *J. Am. Chem. Soc.* **1987**, *109*, 4412; (e) Arnold, D. W.; Xu, C.; Neumark, D. M. *J. Chem. Phys.* **1995**, *102*, 6088.

(10) If not stated otherwise, all thermochemical data have been taken from: (a) Lias, S. G.; Bartmess, J. E.; Liebman, J. F.; Holmes, J. L.; Levin, R. D.; Mallard, W. G. *Gas-Phase Ion and Neutral Thermochemistry, J. Phys. Chem. Ref. Data, Suppl. 1*, 1988; (b) Lias, S. G.; Liebman, J. F.; Levin, R. D.; Kafafi, S. A. *NIST Standard Reference Database, Positive Ion Energetics, Version 2.01*, Gaithersburg, MD, 1994; (c) Bartmess, J. E. *NIST Standard Reference Database, Negative Ion Energetics, Version 3.01*; Gaithersburg, MD, 1993; (d) Lias, S. G.; Liebman, J. F.; Levin, R. D. *J. Phys. Chem. Ref. Data* **1984**, *13*, 695.

(11) McMillen, D. F.; Golden, D. M. *Annu. Rev. Phys. Chem.* **1982**, *33*, 493.

(12) Harvey, J. N.; Aschi, M.; Koch, W.; Schwarz, H. *Theor. Chim. Acta*, in press.

(13) *GAUSSIAN 94, Revision B.3*; Frisch, M. J.; Trucks, G. W.; Schlegel, H. B.; Gill, P. M. W.; Johnson, B. G.; Robb, M. A.; Cheeseman, J. R.; Keith, T.; Peterson, G. A.; Montgomery, J. A.; Raghavachari, K.; Al-Laham, M. A.; Zakrzewski, V. G.; Ortiz, J. V.; Foresman, J. B.; Peng, C. Y.; Ayala, P. Y.; Chen, W.; Wong, M. W.; Andres, J. L.; Replogle, E. S.; Gomperts, R.; Martin, R. L.; Fox, D. J.; Binkley, J. S.; Defrees, D. J.; Baker, J.; Stewart, J. P.; Head-Gordon, M.; Gonzales, C.; Pople, J. A., GAUSSIAN: Pittsburgh, PA, 1992.

(14) (a) Curtiss, L. A.; Raghavachari, K.; Trucks, G. W.; Pople, J. A. *J. Chem. Phys.* **1991**, *94*, 7221; (b) Curtiss, L. A.; Kock, L. D.; Pople, J. A. *J. Chem. Phys.* **1991**, *95*, 4040; (c) Curtiss, L. A.; Raghavachari, K.; Pople, J. A. *J. Chem. Phys.* **1993**, *98*, 1293; (d) For a modification of the G2 approach using DFT, see: Bauschlicher, C. W., Jr.; Partridge, H. *J. Chem. Phys.* **1995**, *103*, 1788.

(15) Kishnan, R.; Binkley, J. S.; Seeger, R.; Pople, J. A. *J. Chem. Phys.* **1980**, *72*, 650.

(16) It should be noted that a failure of DFT methods in the description of van der Waals complexes was reported recently. Therefore, the bond dissociation energy of these complexes may deviate from exact values by a few kcal/mol. This report does not, however, affect the conclusions drawn here (see: Kang, H. C. *Chem. Phys. Lett.* **1996**, *254*, 135). Similar arguments can be applied to the problem of basis set superposition errors that can be assumed to be small for BECKE3LYP.

(17) (a) Galbraith, J. M.; Schaefer III, H. F. *J. Chem. Phys.* **1996**, *105*, 862; For the performance of DFT and HF/DFT methods in the theoretical description of anions and their electron affinities see also: (b) King, R. A.; Galbraith, J. M.; Schaefer, H. F., III *J. Phys. Chem.* **1996**, *100*, 6061; (c) Schalley, C. A.; Schröder, D.; Schwarz, H.; Möbus, K.; Boche, G. *Chem. Ber./Recueil* **1997**, *130*, 1085.

(18) (a) Rauhut, G.; Pulay, R. *J. Phys. Chem.* **1995**, *99*, 3093; (b) Scott, A. P.; Radom, L. *J. Phys. Chem.* **1996**, *100*, 16502.

(19) Gill, P. M. W.; Johnson, B. G.; Pople, J. A. *Chem. Phys. Lett.* **1992**, *197*, 499.

(20) The energetic deviations are just within the error margins of ±5 kcal/mol for the BECKE3LYP/6-311++G(d,p) and ±2 kcal/mol for the G2 calculations. For cumulative deviations in general, see also Nicolaides, N.; Radom, L. *J. Phys. Chem.* **1994**, *98*, 3092.

(21) Fukui, K. *Acc. Chem. Res* **1981**, *14*, 363.

(22) (a) Gonzalez, C.; Schlegel, H. B. *J. Chem. Phys.* **1989**, *90*, 2154; (b) Gonzalez, C.; Schlegel, H. B. *J. Phys. Chem.* **1990**, *94*, 5523.

(23) For a related system see: Hrušák, J.; Iwata, S. *J. Chem. Phys.* **1997**, *106*, 4877.

(24) Koput, J. *J. Mol. Spectrosc.* **1986**, *115*, 438.

(25) For a recent review on CC methods see: Bartlett, R. C. In *Modern Electronic Structure Theory*; Yarkony, D. R., Ed.; World Scientific: Singapore, 1994.

(26) For a discussion of this problem see: (a) Cremer, D.; Gauss, J.; Kraka, E.; Stanton, J. F.; Bartlett, R. J. *Chem. Phys. Lett.* **1993**, *209*, 547; (b) Wierlacher, S.; Sander, W.; Marquardt, C.; Kraka, E.; Cremer, D. *Chem. Phys. Lett.* **1994**, *222*, 319; (c) Kim, S.-J.; Schaefer, H. F., III; Kraka, E.; Cremer, D. *Mol. Phys.* **1996**, *88*, 93; (d) Kraka, E.; Konkoli, Z.; Cremer, D.; Fowler, J.; Schaefer, H. F., III *J. Am. Chem. Soc.* **1996**, *118*, 10595. Furthermore, Hrušák and Iwata (ref 23) stated that for frequency calculations of the $HOOH^{\bullet+}$ cation radical, the MP(*n*) methods fail to calculate the asymmetrical stretchings, whereas "CCSD(T) and surprisingly also the DFT methods ... give reasonable frequencies". Also see: (e) Hrušák, J.; Schröder, D.; Iwata, S. *J. Chem. Phys.* **1997**, *106*, 7541.

(27) (a) Gutbrod, R.; Schindler, R. N.; Kraka, E.; Cremer, D. *Chem. Phys. Lett.* **1996**, *252*, 221; (b) Sander, W.; Schroeder, K.; Muthusamy, S.; Kirschfeld, A.; Kappert, W.; Boese, R.; Kraka, E.; Sosa, C.; Cremer, D. *J. Am. Chem. Soc.* **1997**, *119*, 7265; (c) Gutbrodt, R.; Kraka, E.; Schindler, R. N.; Cremer, D. *J. Am. Chem. Soc.* **1997**, *119*, 7330.

(28) Of course, the rate constant for the spin crossing exit channel does not only depend on energetic criteria but also on the probability of spin inversion, which is a function of the spin−orbit coupling constant H^{SO}.

(29) (a) Butler, J. J.; Holland, D. M. P.; Stockbauer, R. *Int. J. Mass Spectrom. Ion Processes* **1984**, *58*, 1. Similar problems were encountered for the ionization energy of methanol; see (b) Ma, N. L.; Smith, B. J.; Pople,

J. A.; Radom, L. *J. Am. Chem. Soc.* **1991**, *113*, 7903; (c) Schalley, C. A.; Dieterle, M.; Schröder, D.; Schwarz, H.; Uggerud, E. *Int. J. Mass Spectrom. Ion Processes* **1997**, *163*, 101; (d) Also see ref 20. Most recently, a concise treatment appeared in the literature; see: (e) Gauld, J. W.; Glukhovtsev, M. N.; Radom, L. *Chem. Phys. Lett.* **1996**, *262*, 187.

(30) Koller, J.; Hodošcek, M.; Plesnicar, B. *J. Am. Chem. Soc.* **1990**, *112*, 2124.

(31) (a) Sokrates, G. *Infrared Characteristic Group Frequencies*; Wiley: New York, 1980; (b) Hesse, M.; Meier, H.; Zeeh, B. *Spektroskopische Methoden in der Organischen Chemie*; Thieme: Stuttgart, 1991; p 29.

(32) For a discussion of methyl shifts see: Houk, K. N.; Li, Y.; Evanseck, J. D. *Angew. Chem.* **1992**, *104*, 711; ibid, *Angew. Chem., Int. Ed. Engl.* **1992**, *31*, 682.

(33) Bach, R. D.; Ayala, P. Y.; Schlegel, H. B. *J. Am. Chem. Soc.* **1996**, *118*, 12758.

(34) For a NRMS study of ylides see: Wesdemiotis, C.; Feng, R.; Danis, P. O.; Williams, E. R.; McLafferty, F. W. *J. Am. Chem. Soc.* **1986**, *108*, 5847.

(35) For reviews on distonic ions see: (a) Hammerum, S. *Mass Spectrom. Rev.* **1988**, *7*, 123; (b) Stirk, K. M.; Kiminkinen, L. K.; Kenttämaa, H. I. *Chem. Rev.* **1992**, *92*, 1649; (c) Kentämaa, H. I. *Org. Mass Spectrom.* **1994**, *29*, 1; (d) Smith, R. L.; Chou, P. K.; Kenttämaa, H. I. In *The Structure, Energetics and Dynamics of Organic Ions*; Baer, T.; Ng, C. Y.; Powis, I., Eds.; Wiley: New York, 1996; p 197.

(36) (a) Bouma, W. J.; MacLeod, J. K.; Radom, L. *J. Am. Chem. Soc.* **1982**, *104*, 2930; (b) Holmes, J. L.; Lossing, F. P.; Terlouw, J. K.; Burgers, P. C. *J. Am. Chem. Soc.* **1982**, *104*, 2931; (c) Schwarz, H. *Nachr. Chem. Technol. Lab.* **1983**, *31*, 451; (d) Radom, L.; Bouma, W. J.; Nobes, R. H.; Yates, B. F. *Pure Appl. Chem.* **1984**, *56*, 1831.

(37) Schalley, C. A.; Fiedler, A.; Hornung, G.; Wesendrup, R.; Schröder, D.; Schwarz, H. *Chem. Eur. J.* **1997**, *3*, 626.

(38) Schalley, C. A.; Schröder, D.; Schwarz, H. *Int. J. Mass Spectrom. Ion Processes* **1996**, *153*, 173.

(39) Transition structures similar to **TS1**$^{\bullet+}$ are quite typical for organic cation radicals. For example, see (a) Ruttink, P. J. A. In *The Structure of Small Radicals and Ions*; Naaman, R., Vager, Z., Eds.; Plenum: New York, 1981; p 243; (b) Schaftenaar, G.; Postma, R.; Ruttink, P. J. A.; Burgers, P. C.; McGibbon, G. A.; Terlouw, J. K. *Int. J. Mass Spectrom. Ion Processes* **1990**, *100*, 521; (c) Schröder, D.; Sülzle, D.; Dutuit, O.; Baer, T.; Schwarz, H. *J. Am. Chem. Soc.* **1994**, *116*, 6395.

(40) Schalley, C. A.; Schröder, D.; Schwarz, H. *Helv. Chim. Acta* **1995**, *78*, 1999.

(41) For a theoretical study of several nonperoxidic $[C, H_4, O_2]^{\bullet+}$ ion−dipole complexes see: Coitiño, E. L.; Lledos, A.; Serra, R.; Bertran, J.; Ventura, O. N. *J. Am. Chem. Soc.* **1993**, *115*, 9121, and literature cited therein.

(42) For reviews on ion dipole complexes see: (a) Morton, T. H. *Tetrahedron* **1982**, *42*, 6234; (b) Heinrich, N.; Schwarz, H. In *Ion and Cluster Ion Spectroscopy*; Maier, J. P., Ed.; Elsevier: Amsterdam, 1989; p 328; (c) Bowen, R. D. *Acc. Chem. Res* **1991**, *24*, 364; (d) Longevialle, P. *Mass Spectrom. Rev.* **1992**, *11*, 157.

(43) (a) Bouma, W. J.; Nobes, R. H.; Radom, L. *Org. Mass Spectrom.* **1982**, *17*, 315; (b) Burgers, P. C.; Holmes, J. L. *Org. Mass Spectrom.* **1984**, *19*, 452; (c) Aschi, M.; Harvey, J. N.; Schalley, C. A.; Schröder, D.; Schwarz, H. *J. Chem. Soc., Chem. Commun.*, in press.

(44) (a) Bair, R. A.; Goddard, W. A., III *J. Am. Chem. Soc.* **1982**, *104*, 2719; (b) Gase, W.; Boggs, J. E. *J. Mol. Struct.* **1984**, *116*, 207; (c) Christen, D.; Mack, H.-D.; Oberhammer, H. *Tetrahedron* **1988**, *44*, 7363; (d) Huang, M.-B.; Suter, H. U. *J. Mol. Struct.* **1994**, *337*, 173.

(45) Kimura, K.; Osafune, K. *Bull. Chem. Soc. Jpn.* **1975**, *48*, 2421.

(46) (a) Rademacher, P.; Elling, W. *Liebigs Ann. Chem.* **1979**, 1473; (b) Glidewell, C. *J. Mol. Struct.* **1980**, *67*, 35; (c) Haas, B.; Oberhammer, H. *J. Am. Chem. Soc.* **1984**, *106*, 6146.

(47) Schalley, C. A.; Hornung, G.; Schröder, D.; Schwarz, H. *Int. J. Mass Spectrom. Ion Processes*, in press.

(48) For reviews on selected topics in matrix isolation chemistry see: (a) Sander, W. *Angew. Chem.* **1990**, *102*, 362; ibid, *Angew. Chem., Int. Ed. Engl.* **1990**, *29*, 344; (b) Sander, W.; Bucher, G.; Wierlacher, S. *Chem. Rev. (Washington, D.C.)* **1993**, *93*, 1583; (c) Sander, W.; Kirschfeld, A. In *Matrix-Isolation of Strained Three-Membered Ring Systems*; Halton, B., Ed.; JAI: London, 1995; Vol. 4, p 1.

(49) (a) Burgers, P. C.; Holmes, J. L.; Hop, C. E. C. A.; Postma, R.; Ruttink, P. J. A.; Terlouw, J. K. *J. Am. Chem. Soc.* **1987**, *109*, 7315; (b) Yates, B. F.; Bouma, W. J.; MacLeod, J. K.; Radom, L. *J. Chem. Soc., Chem. Commun.* **1987**, 204; (c) Cao, J. R.; George, M.; Holmes, J. L.; Sirois, M.; Terlouw, J. K.; Burgers, P. C. *J. Am. Chem. Soc.* **1992**, *114*, 2017; (d) Audier, H. E.; Milliet, A.; Leblanc, D.; Morton, T. H. *J. Am. Chem. Soc.* **1992**, *114*, 2020; (e) Ruttink, P. J. A.; Burgers, P. C. *Org. Mass Spectrom.* **1993**, *28*, 1087; (f) Suh, D.; Burgers, P. C.; Terlouw, J. K. *Rap. Commun. Mass Spectrom.* **1995**, *9*, 862.

(50) Fraser, R. T. M.; Paul, N. C.; Philips, L. *J. Chem. Soc. (B)* **1970**, 1278.